Chapter 3
Monopole Sources

3.1 The Mathematical Model

First, mathematical models of the monopole are developed to provide as much useful information as possible. Then real applications are discussed and analyzed with use of the mathematical model and the scaling rules.

The basic wave equation for the monopole has spherical symmetry.

$$\frac{\partial}{\partial\theta}=0,\frac{\partial}{\partial\psi}=0$$
$$\frac{\partial}{\partial r^2}(r\phi)-\frac{1}{c_0^2}\frac{\partial}{\partial t^2}(r\phi)=0 \qquad (3.1)$$
$$\frac{\partial}{\partial r^2}(r\Phi)+k^2(r\Phi)=0$$

φ(r, t) and **Φ(r, ω)** are the velocity potentials. The general solution in the time domain is that any continuous but arbitrary function satisfies the wave equation and is propagated radially outward in time without change of form as shown in the first of Eqs. 3.2. The single frequency solution is given in the second equation.

$$\phi(r,t)=\frac{1}{4\pi r}f\left(t-\frac{r}{c_0}\right)$$
$$\phi(r,t)=\frac{Q_m}{4\pi r}e^{i(\omega t-kr)} \qquad (3.2)$$

The main variables are

$$p(r,t)=\rho_0\frac{\partial\phi}{\partial t} \qquad u_r(r,t)=-\frac{\partial\phi}{\partial r} \qquad u_\theta=u_\psi=0$$

3.1.1 Physical Interpretation of the Source

To properly model the monopole it is necessary to look at the equations as representative of a physical process. Consider the source as an arbitrary function of time; by use of the Helmholtz equation we get

$$\Phi(r,\omega)=\frac{q_m(\omega)}{4\pi r}e^{-ikr}$$
$$q_m(\omega)=\int_{-\infty}^{\infty}Q_m(t)e^{-i\omega t}dt \qquad (3.3)$$
$$Q_m(t)=\frac{1}{2\pi}\int_{-\infty}^{\infty}q_m(\omega)e^{i\omega t}d\omega$$

The source spectrum is defined by the Fourier transform pair. By making use of the shifting theorem the time dependent value of the velocity potential becomes

$$\phi(r,t)=\frac{1}{2\pi}\int_{-\infty}^{\infty}\Phi(r,\omega)e^{i\omega t}d\omega=\frac{1}{4\pi r}\left[\frac{1}{2\pi}\int_{-\infty}^{\infty}q_m(\omega)e^{i\omega\left(t-\frac{r}{c_0}\right)}d\omega\right]=\frac{Q_m\left(t-\frac{r}{c_0}\right)}{4\pi r}$$

Although this result seems trivial, it leads to some interesting results. The physical variables are

$$p(r,t)=\frac{\rho_0}{4\pi r}\frac{\partial Q_m\left(t-\frac{r}{c_0}\right)}{\partial t}$$

$$u_r(r,t)=\frac{1}{4\pi r c_0}\left[\frac{\partial Q_m\left(t-\frac{r}{c}\right)}{\partial t}+\frac{c_0}{r}Q_m\left(t-\frac{r}{c_0}\right)\right]$$

$$I_m(r)=\overline{pu_r}=\frac{Z_0}{16\pi^2r^2c_0^2}\left[\overline{\frac{\partial Q_m}{\partial t}*\frac{\partial Q_m}{\partial t}}+\overline{Q_m*\frac{\partial Q_m}{\partial t}}\right]$$

The time retardation factor was left out of the intensity expression for simplicity. The bars represent the time average. The second term in the velocity and intensity expressions represents the reactive motion near the source. By putting the mean fluid density into the expression, the resistive part of the radial intensity becomes

$$I_m(r)=\frac{Z_0}{16\pi^2r^2c_0^2}\overline{\left(\frac{\partial Q_m}{\partial t}\right)^2}=\frac{1}{16\pi^2r^2Z_0}\overline{\left(\frac{\partial \dot{M}}{\partial t}\right)^2} \tag{3.4}$$

$\dot{M}$ is the mass flow rate. The sound power can be expressed simply as

$$W=\frac{1}{4\pi Z_0}\overline{\left(\frac{\partial \dot{M}}{\partial t}\right)^2} \tag{3.5}$$

The sound from a monopole is created by the mean square of the time rate of change of the mass flow rate.

3.2 The Single Frequency Point Monopole

3.2.1 Physical Variables

A solution of the wave equation for a single frequency can be expressed in terms of the velocity potential {A.3.1} as shown in the first of Eqs. 3.6. There is an incoming wave solution also, but that has been discarded since we are interested in radiating sources. The quantity $\mathbf{Q_m}$ is called the *source strength* and a check of units will show that it has the dimensions $\mathbf{L^3/T}$, a volumetric flow rate. Several of the physical variables are also shown below in terms of the velocity potential.

$$\begin{aligned}
&\phi(r,t) = \frac{Q_m}{4\pi r} e^{i(wt-kr)} && \xi_r(r,t) = \frac{(kr-i)}{krc_0}\phi \\
&p(r,t) = \frac{ikZ_0Q_m}{4\pi r} e^{i(\omega t-kr)} = ikZ_0\phi && s(r,t) = \frac{ik}{c_0}\phi \\
&u_r(r,t) = \frac{(1+ikr)}{r^2} * \frac{Q_m}{4\pi} e^{i(\omega t-kr)} = \frac{(1+ikr))}{r}\phi && T(r,t) = \frac{i\omega}{R}\left(\frac{\gamma-1}{\gamma}\right)\phi \\
&a_r(r,t) = \frac{ikr}{c_0}\frac{(1+ikr)}{r^2}\phi
\end{aligned} \qquad (3.6)$$

The scalar quantities, pressure **p**, temperature **T**, and condensation **s** remain in phase as expected. The radial acceleration $\mathbf{a_r}$, velocity $\mathbf{u_r}$, and displacement $\boldsymbol{\xi_r}$ are at quadrature with each other. Depending on radius, the radial velocity can be either in phase with the pressure or at quadrature with it. This is related to the compressible-incompressible flow regions around the source. The close-in region is called the *near sound field* and the other the *far sound field.*

It is possible to define *local* Strouhal and Mach numbers as shown on the right. The characteristic speed is the "particle" speed and the characteristic length radial distance. Note that the local Strouhal number increases with radius and the local Mach number decreases with radius, i.e., the validity of the wave equation improves with radius {D.2}.

$$St_s = \frac{fr}{|u_r|}, Ma_s = \frac{|u_r|}{c_0}$$

3.22 Near Field

Close to the origin, the radial acceleration is nearly in phase with the pressure; the pressure is used primarily to accelerate the fluid; the motion is reactive and essentially incompressible. Since the velocity is at quadrature with the pressure, very little work is being

$$\begin{aligned}
p(r,t) &= \frac{ikZ_0Q_m}{4\pi r} e^{i(\omega t-kr)} \\
u_r(r,t) &= \frac{Q_m}{4\pi r^2} e^{i(\omega t-kr)} \\
a_r(r,t) &= \frac{ikQ_m}{4\pi r^2 c_0} e^{i(wt-kr)}
\end{aligned}$$

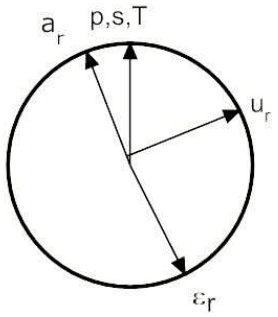

done on the medium. The sound field is a smaller part of the motion.

3.2.3 Far Field

Far from the origin the phase of the velocity shifts to be the same as the scalar variables. The reactive motion is minimized, and work is being done on the medium. The sound field is dominant.

$$p(r,t) = \frac{ikZ_0 Q_m}{4\pi r} e^{i(\omega t - kr)}$$

$$u_r(r,t) = \frac{ikQ_m}{4\pi r} e^{i(\omega t - kr)}$$

$$a_r(r,t) = -\frac{k^2 Q_m}{4\pi r c_0} e^{i(wt - kr)}$$

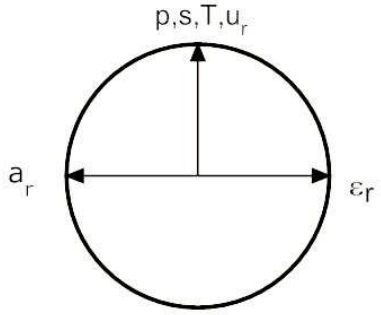

3.2.4 Radiation Impedance

The impedance to radial motion has both reactive and resistive components. Close to the source the reactive (incompressible) components dominate. Further out the resistive (sound field) components dominate. The impedance can be expressed in several ways as shown below.

$$Z_r = \frac{p}{u_r} = Z_0 \frac{ikr}{(1+ikr)} = Z_0 \frac{kr}{\sqrt{1+k^2r^2}} e^{i\left(\frac{\pi}{2}-\alpha\right)} = R_m + iX_m$$

$$\tan\alpha = kr$$

$$R_m = Z_0 \frac{k^2r^2}{1+k^2r^2}, X_m = Z_0 \frac{kr}{1+k^2r^2}$$

3.2.5. Sound Intensity

The power flow per unit area, or intensity, is purely radial. It is

$$I_r(r) = p \bullet u_r^* = \frac{k^2 Z_0 Q_m^2}{16\pi^2 r^2}\left[1 + \frac{i}{kr}\right] \qquad (3.7)$$

At large kr (not **r** alone) the pressure and velocity are in phase as in the plane wave case; the *sound intensity* is the real part of the expression. For a given volumetric flow rate, the intensity increases with the square of the frequency, decreases with the square of the distance, and increases with the impedance of the medium.

Looking at the reactive part of the intensity, we see that it decreases with the cube of the distance, suggesting that it is more like an incompressible flow field. It is reasonable to set the near/far field boundary at **kr = 10**. The radius of the boundary decreases with increasing frequency, suggesting a smaller reactive volume at high frequencies.

Key Points: In some documents, the denominator has 8 in Eq. 3.7, in lieu of 16, because the value of $\mathbf{Q_m}$ was described as the peak amplitude while here it is described as the r.m.s.

amplitude, the difference of the squares being two {A.2}. This also applies to the sound power equation below {3.2.7}.

3.2.6 Estimates of Sound Intensity

Direct intensity measurements and their integral to estimate sound power require specialized equipment. How well does a sound pressure measurement approximate to intensity? The relationship for this is

$$EST\left[I_r\right] = \frac{p \bullet p^*}{Z_0} = \frac{k^2 Z_0 Q_m^2}{16\pi^2 r^2} \tag{3.8}$$

A mean square pressure measurement will represent the intensity correctly, despite the presence of some incompressible flow (provided, of course, that the source is in fact a monopole). The sound pressure level and source strength are

$$L_p = 10Log_{10}\left[\frac{k^2 Z_0^2 Q_m^2}{16\pi^2 r^2 p_R^2}\right]$$

$$Q_m = \frac{2rp_R c_0}{fZ_0} 10^{\frac{L_p}{20}}$$

The following relationships result:

6 dB/octave increase per doubling of frequency
6 dB increase per doubling of source strength
6 dB decrease per doubling of distance

Note that the above results imply that the sound level will increase indefinitely with frequency - pure nonsense. At some point, the wavelength will be on the order of the actual source size. This is taken into account in {3.3} below. In many practical cases, this is not an issue, but it is important to be aware of this limitation {6.1.4}.

3.2.7 The Sound Power

The power is the integral of intensity over the sphere

$$W_m = \int_0^{2\pi}\int_0^{\pi} I_r\left(r\right) r^2 \sin\vartheta d\vartheta d\psi = 4\pi r^2 I_r\left(r\right) = \frac{k^2 Z_0 Q_m^2}{4\pi} \tag{3.9}$$

The acoustic power is the real part of the expression. Again, we see that the wave equation cannot be correct for a truly point source since the *reactive* power requirements tend toward infinity as **r** approaches zero {6.1.1}.

3.2.8 Dimensional Analysis

By introducing dimensionless factors into the sound power equation, it can be presented in a different form by adding the characteristic length **L** and speed **U** (undefined at this point).

$$W_m = \frac{\pi\rho_0}{c_0}\hat{Q}^2 St^2 U^4 L^2$$
$$\hat{W}_m = \pi\hat{Q}^2 St^2 M \tag{3.10}$$

Definitions of the dimensionless variables are in {A.2.2}. This equation applies for a single frequency point monopole. It can also apply for a single frequency finite monopole whose radius is much less than a wavelength {3.3.3}, i.e., the Helmholtz number is much less than one {A.2.2.2}.

3.3 The Single Frequency Finite Monopole (Pulsating Sphere)

3.3.1 The Physical Variables

All of 3.2 is useful but still fiction; real sources have finite dimensions. Note that for the point monopole the volumetric flow rate remains constant despite the zero size of the source. Worse, the sound pressure increases as the square of the frequency ad infinitum. As the source is approached, the radiation impedance goes to zero. It is clear that the approximations made to develop the wave equation must of necessity be invalid for small values of the radius {6.1.1}. Consider a situation closer to reality, a monopole of finite size; a pulsating sphere of radius **a**. The boundary conditions on the surface of the sphere determine the resulting sound field. The radial velocity on the surface of the sphere is related to the volumetric flow rate as

$$u_r(a,t) = u_a e^{i\omega t}$$
$$Q_m = 4\pi a^2 u_a \tag{3.11}$$

Since the surface of the sphere and fluid immediately in contact with it must have the same motion, the Mach number of the velocity must be small {2.3.3}. In the point source solution, the phase was chosen with respect to r=0 and now it must be chosen with respect to r=a. The important variables become

$$\phi(r,t) = \frac{1}{1+ika}\frac{Q_m}{4\pi r}e^{i(\omega t - k(r-a))}$$
$$p(r,t) = \frac{ika}{1+ika}\left(\frac{a}{r}\right)Z_0 u_a e^{i(\omega t - k(r-a))} \tag{3.12}$$
$$u_r(r,t) = \frac{1+ikr}{1+ika}\left(\frac{a}{r}\right)^2 u_a e^{i(\omega t - k(r-a))}$$

3.3.2 Near Field

For **kr<<1**, the following expressions apply. The radial velocity grows as the square of the distance as the source is approached and is at quadrature with the pressure, suggesting the dominance of the incompressible flow field.

$$p(r,t) = \frac{ika}{1+ika}\left(\frac{a}{r}\right)Z_0 u_a e^{i(\omega t - k(r-a))}$$

$$u_r(r,t) = \frac{1}{1+ika}\left(\frac{a}{r}\right)^2 u_a e^{i(\omega t - k(r-a))}$$

3.3.3 Far Field

For **kr>>1**, the following expressions apply. The radial velocity and pressure are in phase and each decrease linearly with distance.

$$p(r,t) = \frac{ika}{1+ika}\left(\frac{a}{r}\right)Z_0 u_a e^{i(\omega t - k(r-a))}$$

$$u_r(r,t) = \frac{ikr}{1+ika}\left(\frac{a}{r}\right)^2 u_a e^{i(\omega t - k(r-a))}$$

3.3.4 Source Size

For a source that is large with respect to the radiated frequency (**ka>>1**), the following expressions apply. This would be a very rare occasion. Note that frequency dependence is lost; the source is more like a plane source.

$$p(r,t) = \left(\frac{a}{r}\right)Z_0 u_a e^{i(\omega t - k(r-a))}$$

$$u_r(r,t) = \left(\frac{a}{r}\right)u_a e^{i(\omega t - k(r-a))}$$

3.3.5 Radiation Impedance

The radial impedance at the surface of a finite sized sphere is

$$Z_a = Z_0 \frac{ika}{1+ika} = R_a + iX_a$$

$$R_a = Z_0 \frac{k^2 a^2}{1+k^2 a^2} \qquad (3.13)$$

$$X_a = Z_0 \frac{ka}{1+k^2 a^2}$$

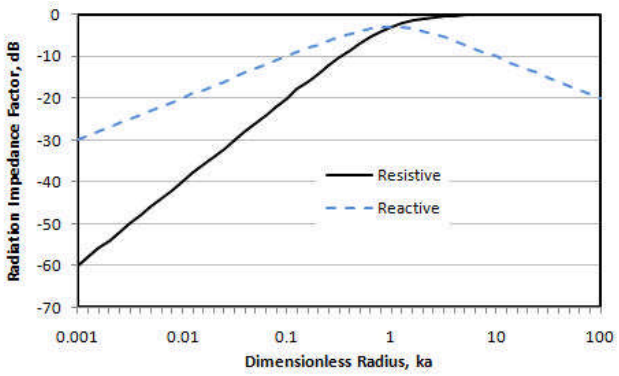

Fig. 3-1. Finite monopole impedance.

The radiation resistance increases with the square of the frequency as with the point monopole, but as **ka** approaches one, it becomes limited, bringing the results closer to reality. Both resistance and reactance are 3 dB down when the Helmholtz number is one (**ka=1)**. The *acoustical* Strouhal number is 0.16, based on the characteristic length being the source radius **a,** and the characteristic speed being $\mathbf{c_0}$. At low frequencies, the resistive impedance increases at 6 dB/octave while the reactive impedance increases at 3 dB/octave. The hydrodynamic motion (fluid acceleration) dominates at low frequencies while at high frequencies the acoustic motion (fluid compression) dominates.

Key Points: For a given volumetric (mass) flow rate, sound output increases with frequency so frequency reduction (speed, RPM) will reduce output. The impedance applies to broadband sources, so the radiated spectrum at very high frequencies will not be the same as the initiating spectrum at the source.

3.3.6 Sound Intensity

The sound intensity is given in Eqs. 3.14. The reactive component decays with distance more rapidly than the resistive. Note again that for a source large with respect to a wavelength, there is no frequency dependence, the impedance maximizes at some point, as suggested in Figure 3-1.

$$I_r(r,t) = u_a^2 Z_0 \left[\left(\frac{a}{r}\right)^2 \frac{k^2a^2}{1+k^2a^2} + i\left(\frac{a}{r}\right)^3 \frac{ka}{1+k^2a^2} \right]$$

$$I_r(r,t) = \frac{Z_0 Q_m^2}{16\pi^2\left(1+k^2a^2\right)} \left[\frac{k^2}{r^2} + i\frac{k}{r^3} \right] \qquad (3.14)$$

3.3.7 Estimates of Sound Intensity

Direct intensity measurements and their integral to estimate sound power require specialized equipment. How well does a sound pressure measurement approximate to far field intensity? The relationship for this is

$$EST\left[I_r\right] = \frac{p \bullet p^*}{Z_0} = u_a^2 Z_0 \left(\frac{a}{r}\right)^2 \frac{k^2a^2}{1+k^2a^2} \qquad (3.15)$$

A mean square pressure measurement will represent the far field intensity correctly, despite the presence of some incompressible flow (provided, of course, that the source is in fact a monopole).

3.3.8 Sound Power

The sound power can be expressed in a simple way. For a given surface velocity, the sound power increases with the sphere's surface area $\mathbf{A_s}$, as expected.

$$W_m = 4\pi r^2 I_r = \frac{Q_m^2 k^2 Z_0}{4\pi\left(1+k^2a^2\right)} = 4\pi a^2 u_a^2 Z_0 \frac{k^2a^2}{\left(1+k^2a^2\right)} = A_s u_a^2 R_m \qquad (3.16)$$

3.3.9 Dimensional Analysis

Eq. 3.16 is the same as for a point monopole (Eq. 3.10) when **ka<<1**. When **ka>>1**, the form of Eq. 3.11 must be altered as shown below. The speed dependence is reduced, the sound power is no longer dependent on frequency, and the characteristic length is now defined. This equation applies only for high frequencies, since the value of **ka** implies wave lengths that are quite short with respect to the radius. It is likely that such a case occurs rarely. For broad-band sound, the change in speed dependence of the high frequency components will distort the spectrum; this is discussed in {6.1.4}.

For a finite monopole with a very large radius with respect to wavelength, the dependence on the steady speed changes from $\mathbf{U^4}$ to $\mathbf{U^2}$ as shown below

$$W_m = \frac{Z_0}{4\pi}\hat{Q}^2 U^2 a^2$$

3.4 The Interaction of Two Single Frequency Finite Monopoles

3.4.1 The Mathematical Model

Consider two monopoles of equal size separated by a distance **2h**. The velocity potential at the measurement point is the sum of each as shown in Eq. 3.17. The variable δ is an arbitrary phase angle between the sources. The measurement angle starts at the vertical.

$$\phi(r,t) = \frac{1}{1+ika}\frac{Q_{m1}}{4\pi r_1}e^{i(\omega t - k(r_1 - a))} + \frac{1}{1+ika}\frac{Q_{m2}}{4\pi r_2}e^{i(\omega t - k(r_2 - a) + \delta)} \qquad (3.17)$$

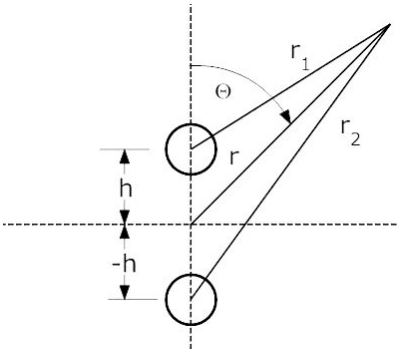

Fig. 3-2. Geometry.

The first of Eqs. 3.18 below represents the sound pressure at the measurement point in terms of the radial velocities of each source. The second two equations below relate the actual distances to that from the coordinate center. A helpful approximation is that the distances from the sources is large with respect to the distance between the sources, i.e., **r>>>2h**. This is properly called the *geometric far field* and is not related to any wavelength. The approximation is typically incorporated in the phase term but the difference in distances is often neglected to simplify calculations. The terms in red are second order approximations and are neglected. As a result, the amplitude and distance differences limit the validity of the approximation {6.1.3}.

$$p(r,t) = \frac{ika}{1+ika} Z_0 a e^{i\omega t}\left[\frac{u_{m1}}{r_1}e^{-ikr_1} + \frac{u_{m2}}{r_2}e^{-ikr_2+\delta}\right] \tag{3.18}$$

$$r_1 = \sqrt{r^2+h^2-2rhCos\theta} \approx r + \frac{h^2}{2r} - h\cos\theta$$

$$r_2 = \sqrt{r^2+h^2+2rh\cos\theta} \approx r + \frac{h^2}{2r} + h\cos\theta$$

3.4.2 The Sound Intensity and Sound Power

With these approximations, the mean square pressure, intensity, and power expressions are

$$pp^* = \frac{k^2a^2}{1+k^2a^2}\left(\frac{a}{r}\right)^2 Z_0^2 u_{m1}^2\left[1+\left(\frac{u_{m2}}{u_{m1}}\right)^2 + \frac{2u_{m2}}{u_{m1}}\cos\left(2kh\cos\theta-\delta\right)\right]$$

$$I_r(r,t) = \frac{k^2a^2}{1+k^2a^2}\left(\frac{a}{r}\right)^2 u_{m1}^2 Z_0\left[1+\left(\frac{u_{m2}}{u_{m1}}\right)^2 + \frac{2u_{m2}}{u_{m1}}\cos(2kh\cos\theta-\delta)\right] \tag{3.19}$$

$$W = \frac{k^2a^2}{1+k^2a^2} Z_0 A_s u_{m1}^2\left[1+\left(\frac{u_{m2}}{u_{m1}}\right)^2 + \frac{2u_{m2}}{u_{m1}}\frac{\sin(2kh)}{2kh}\cos\delta\right]$$

The symbol $\mathbf{A_s}$ represents the surface area of the sphere $4\pi a^2$. If the second source is absent, the single source equation is recovered. Consider two extreme cases where the separation of the sources is small: one where they are in phase and the second where they are in opposition. The bracket terms degenerate to those shown on the right. The sound power is either quadrupled when the in-phase sources are close or cancelled when the sources are in opposite phase. The ratio of the sound power of two nearby monopoles to that of a single monopole is shown in the figures. In Figure 3-3, the sources are in phase but are of differing amplitude. In Figure 3-4, the sources are of equal amplitude, but vary in phase in 22.5 degree increments. These particular examples are for the case when **ka<<1**, so the sources act similar to point monopoles.

$[u_{m1}+u_{m2}]^2$

$[u_{m1}-u_{m2}]^2$

There are several interesting results. Consider amplitude. The minimum sound power occurs when the separation distance is $2kh = 11\pi/8$ for sources of equal amplitude, and the

reduction is 4 dB. Consider phase. Whenever the phase angle between the two sources is an odd multiple of 90 degrees, the sources add independently. It is useful to note that in {C.2} the simple diagram for the correlation of random sources shows that sources add independently whenever the correlation coefficient is zero. Phase quadrature qualifies as no correlation. The minimum output occurs at the same separation distance as for the amplitudes.

What is wrong with this analysis? The development of the equations was straightforward but the results do not coincide with reality; real sources are finite. In this mathematical exercise when the two sources merge the volumetric flow rates merge, so we must deal with their square and the sound power must quadruple. Compare this result with two finite pulsating spheres. The first flaw is that the sound from one source can pass through the body of the second. This would not be a severe handicap if the sources were very small with regard to a wavelength and the separation was large; it would be equivalent to a low frequency plane wave diffracting around a sphere. As the sources approach each other, the shadowing and scattering becomes significant. Further, it certainly is not possible to merge one physical sphere with another. Therefore the graphs above are decidedly incorrect for small values of **2kh** and certainly for separations where **h~a.** The region of increased invalidity will lie to the left of the dashed lines in Figures 3-3 and 3-4. Despite this limitation, the analysis provides some insight on the interaction process.

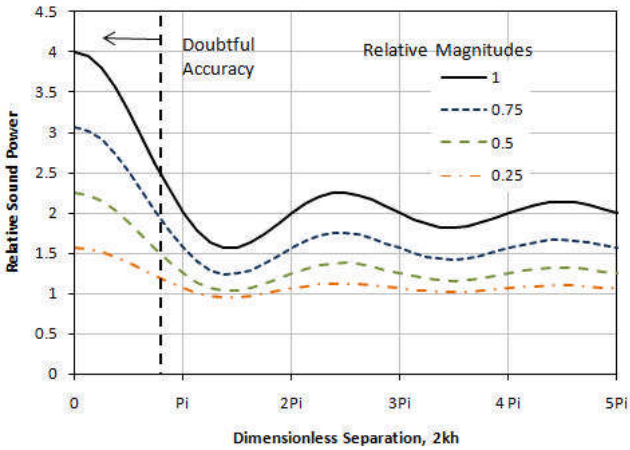

Fig. 3-3. Relative magnitudes of two interacting monopoles.

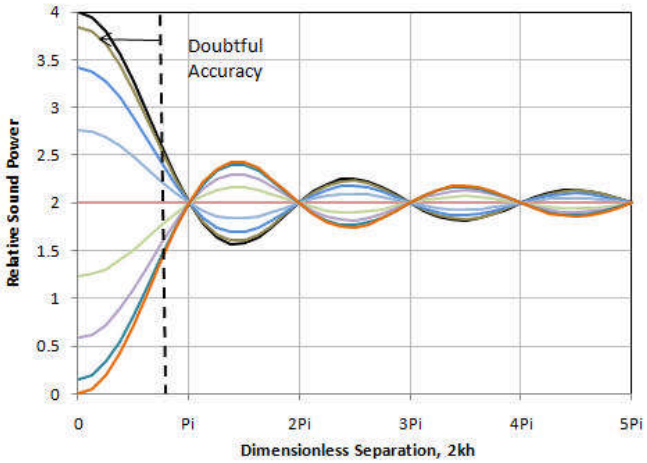

Fig. 3-4. Relative phase of two interacting monopoles.

Directivity patterns are calculated and displayed in the **SoundSource** program for either a single frequency or broad-band spectrum in one third octave bands. The following are the important variables:

Separation distance
Measurement distance
Relative level
Relative phase
Source diameter
Source velocity

The geometric far field approximation is not necessary in the software, so the measurement distance can be closer, but is restricted to distances that avoid the other restrictions noted above. The separation distance is also restricted to four times source size.

3.4.3 The Monopole above a Reflecting Plane

Often, the method above is used to determine the sound field above a reflecting *plane*. The *method of images* is used; the image source is set below the plane so that the boundary conditions on the reflecting plane are met. To do this the image source must have the same phase as the real source. For a hard surface, the amplitude of the two sources must also be equal, resulting in *specular* reflections (angle of incidence equals angle of reflection) and not *diffuse* reflections. The same cautions about the validity of the geometric far field must be applied to this model as well. The integration for sound power is done only for the real hemisphere resulting in the sound power equation for a hard reflecting surface below.

$$W = \frac{k^2a^2}{1+k^2a^2} Z_0 A_s u_{m1}^2 \left[1 + \frac{\sin(2kh)}{2kh} \cos\delta \right] \tag{3.20}$$

In real situations that surface may be an essentially rigid solid or an elastic fluid with a lesser impedance. If that impedance is not infinite, as assumed above, the normal velocity will *not* be zero. For example, a monopole may be either above or below a water surface. Not only will be impedance be finite, but the surface will support surface waves making the above equation only a first approximation. Again, the distance limitation of {3.4.3} applies here.
Key Point: If the source is *in* the plane, the integration of the two sources is complete and the results of {3.10.2} apply.

3.4.4 Two Interacting Square Wave Monopoles

Fourier analysis is applied to a square wave to create a sound source with multiple frequencies. This case can be considered as a periodic volumetric flow with high output such as a loud motorcycle exhaust, so it might be approximated by a square wave. The sound pressure appears as

$$p(r,t) = \sum_{n=1}^{L} \frac{inka}{1+inka} \frac{a}{r_1} Z_0 u_{m1} e^{in(\omega t - kr_1)} + \sum_{m=1}^{L} \frac{imka}{1+imka} \frac{a}{r_2} Z_0 u_{m2} e^{im(\omega t - kr_2)+i\delta} \tag{3.21}$$

For the square wave the sums are over *odd* values only. Since each of the harmonics are phase matched with the fundamental, the phase term is not part of the summation. It was presumed that the surface velocity was a square wave so the harmonics decay as **1/n**. Writing equations for the intensity and power is possible but not informative. Instead, the mean square pressure has been calculated in the **SoundSource** program to show how the higher harmonics create more variations in level than would be the case for a single frequency.
Key Point: In this case there are multiple frequencies that a phase related (coherent) to the fundamental frequency and of declining amplitude. It results in more variations of output with **2kh** than is found in Figure 3-3. The presence of summations makes programming the equation a straightforward matter. For two interacting broadband monopoles, each of the frequencies add incoherently so the variations of output with **2kh** are diminished.

3.5 The Broad-band Point Monopole

It is necessary to work in the frequency domain for this case. Eq. 3.22 is an outgoing solution of the wave equation.

$$\Phi(r,\omega)=\frac{Q_m(\omega)}{4\pi r}e^{-ikr} \tag{3.22}$$

There is little new in these results when compared with the single frequency point monopole except that one works with a broad-band spectrum. The spectrum of the sound field is similar to that of the source.

3.6 The Broad-band Finite Monopole (Vibrating Sphere)

3.6.1 The Physical Variables

The radius of the sphere is **a**. The radial velocity and volumetric flow rate spectrum at the surface is

$$\begin{aligned} u_r(a,\omega)&=U_a(\omega)\\ Q_m(\omega)&=4\pi a^2U_a(\omega)\end{aligned} \tag{3.23}$$

This leads to the following relationships

$$\begin{aligned} \Phi(r,\omega)&=U_a(\omega)\left(\frac{a}{r}\right)^2\frac{1}{1+ika}e^{-ik(r-a)} \qquad u_r(r,\omega)=U_a(\omega)\left(\frac{a}{r}\right)^2\frac{1+ikr}{1+ika}e^{-ik(r-a)}\\ p(r,\omega)&=U_a(\omega)Z_0\left(\frac{a}{r}\right)\frac{ika}{1+ika}e^{-ik(r-a)} \qquad I_r(r,\omega)=U_a^2(\omega)Z_0\left(\frac{a}{r}\right)^2\frac{k^2a^2}{1+k^2a^2}\end{aligned} \tag{3.24}$$

The intensity shown is the far sound field approximation. The radiation impedance remains the same as for the single frequency case. The equations are more complex spectrally, but the results are similar to the single frequency case.

3.6.2 Dimensional Analysis

By introducing dimensionless factors into the sound power equation as was done in {3.2.8}, the sound power can be presented in the following form.

$$\begin{aligned} W_m(\omega)&=\frac{\pi\rho_0}{c_0}\left[\hat{Q}(\omega)S(\omega)\right]^2U^4L^2\\ \hat{W}_m(\omega)&=\pi\left[\hat{Q}(\omega)S(\omega)\right]^2M\end{aligned} \tag{3.25}$$

Again, the characteristic length and speed must be interpreted as fixed values, such as mean flow speed while the dimensionless ratios represent a spectrum. It is necessary to integrate over the frequency dependent terms in the square brackets to obtain the overall sound power. There is

now not only a source strength spectrum, but also a Strouhal number spectrum. In many cases related to flow, these are dependent on Reynolds number.

3.7 Two Interacting Random Point Monopoles

The relationships for this case are

$$\begin{aligned}
\Phi(r,\omega) &= \frac{e^{-ikr}}{4\pi r}\left[Q_{m1}(\omega)e^{ikh\cos\theta} + Q_{m2}(\omega)e^{-ikh\cos\theta}\right] \\
p(r,\omega) &= \frac{ikZ_0e^{-ikr}}{4\pi r}\left[Q_{m1}(\omega)e^{ikh\cos\theta} + Q_{m2}(\omega)e^{-ikh\cos\theta}\right] \\
u_r(r,\omega) &= \frac{\left(1+ikre^{-ikr}\right)}{4\pi r^2}\left[Q_{m1}(\omega)e^{ikh\cos\theta} + Q_{m2}(\omega)e^{-ikh\cos\theta}\right] \\
I_r(r,\omega) &= pu_r^* = \frac{k^2Z_0}{16\pi^2r^2}\left[1+\frac{i}{kr}\right][\ ][\ ]^* \\
[\ ][\ ]^* &= Q_{m1}^2(\omega)\left[1+\frac{Q_{m2}^2(\omega)}{Q_{m1}^2(\omega)} + 2\frac{Q_{m1}(\omega)Q_{m2}(\omega)}{Q_{m1}^2(\omega)}\cos(kh\cos\theta)\right]
\end{aligned} \tag{3.26}$$

The geometric far field approximations of Eqs. 3.18 have been made. It is necessary to integrate the frequency spectrum to get the overall intensity. With band-limited white noise as an example {C.7} the equation is

$$I_r(r)\frac{Z_0}{16\pi^3r^2c_0^2}\left[S_1\int_{L_1}^{L_2}\omega^2d\omega + S_2\int_{L_1}^{L_2}\omega^2d\omega + S_{12}\int_{L_1}^{L_2}\omega^2\cos\left(\frac{\omega h\cos\theta}{c_0}\right)d\omega\right] \tag{3.27}$$

The results are quite complicated and are reserved for the **SoundSource** program. If the second source, $\mathbf{S_2}$, is absent we recover the usual spectrum of the monopole. If the second source, $\mathbf{S_2}$, is equal to the first source, $\mathbf{S_1}$, and they are incoherent ($\mathbf{S_{12}=0}$), the third term is missing and the first two integrals are equal. Some special cases are listed below.

Single Source Case (S_2=0)

$$I_r(r)\frac{Z_0}{16\pi^3r^2c_0^2}\left[S_1\int_{L_1}^{L_2}\omega^2d\omega\right] \tag{3.28}$$

Two Equal Sources, but Incoherent (S_1= S_2, S_{12}=0)

$$I_r(r)\frac{Z_0}{16\pi^3r^2c_0^2}\left[2S_1\int_{L_1}^{L_2}\omega^2d\omega\right]$$

Two Equal, Positively Coherent Sources (S_1= S_2, S_{12}= S_1)

$$I_r(r)\frac{Z_0}{16\pi^3r^2c_0^2}\left[2S_1\int_{L_1}^{L_2}\omega^2d\omega + S_1\int_{L_1}^{L_2}\omega^2\cos\left(\frac{\omega h\cos\theta}{c_0}\right)d\omega\right]$$

Two Equal, Negatively Coherent Sources ($S_1 = S_2$, $S_{12} = -S_1$)

$$I_r(r)\frac{Z_0}{16\pi^3 r^2 c_0^2}\left[2S_1\int_{L_1}^{L_2}\omega^2 d\omega - S_1\int_{L_1}^{L_2}\omega^2\cos\left(\frac{\omega h\cos\theta}{c_0}\right)d\omega\right]$$

The broad-band point monopole case is presented in **SoundSource** for a source above a hard reflecting plane and in the corner of two hard reflecting surfaces. The sound pressure level as a function of angle in a quadrant is shown for a variety of physical values.

Key Points: The sound intensity of two interacting random monopoles is a complicated function of the spectrum of the sources. The examples above are limited examples only. The correlation between the sources largely determines the intensity.

3.8 Fluid Mechanical Estimates of Monopole Directivity

The big flaw in modeling the monopole is that real sources are seldom spherically symmetric, bubble, balloons, and explosions being notable exceptions. Deviations from symmetry can be estimated in two ways. In this section, the motion near the source is viewed as a streamlined fluid flow while in {3.9} known deviations from symmetry are used as models. Streamlines are normally defined for incompressible flows {1.2.3} and in many cases incompressible flow is dominant near the source. In essence, near the source the fluid mechanical Strouhal number $\left[St_1 = \left(\frac{fr}{U}\right)\right]$ is more important than the acoustical Strouhal number. $\left[St_2 = \frac{fr}{c_0} = St_1 M\right]$ By looking at the oscillatory streamlines near the source, it is possible to get an *estimate* of directivity which can be helpful in outdoor propagation. The concept is as follows. The radial component of the streamlines represents the resistive flow that results in sound. Streamlines that are primarily tangential, represent reactive flow and little sound. Streamlines that diverge more than others represent lower levels of sound in the relevant direction, while those that converge, or diverge slowly, represent higher levels of sound. Below are several examples.

3.8.1 A Free Monopole

The flow in and outward from a spherical sound source is spherically symmetric as suggested in Figure 3-5. There is no preferred direction, so the sound field can be estimated to be directionally uniform. The decrease of sound pressure level with distance is suggested by the divergence of the streamlines. These obvious comments are intended as a prelude to more complicated geometries.

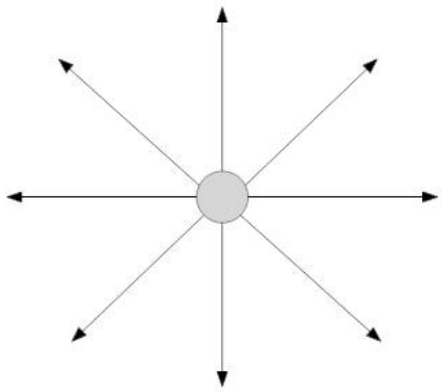

Fig. 3-5. The free monopole streamlines.

3.8.2 A Monopole near a Reflecting Surface

The streamlines in this example show the relationship between the near field flow and the sound field. The streamlines are shown in Figure 3-6, while the calculated sound field is shown in Figure 3-7. The calculation was for a source 2 inches in diameter, 8 inches from the surface, with at frequency of 380 Hz. The streamlines along the surface diverge more slowly than those vertical to the surface, and suggest higher levels along the surface. In the present example, there was nearly a **15 dB** deviation from a perfect monopole source. An argument for the invalidity of such a simple streamline approach is the presence of lobes at higher frequencies due to wave cancellations. In many practical situations, the frequency is sufficiently low that lobes do not appear. In every case there still would be a maximum along the surface as suggested by the streamlines.

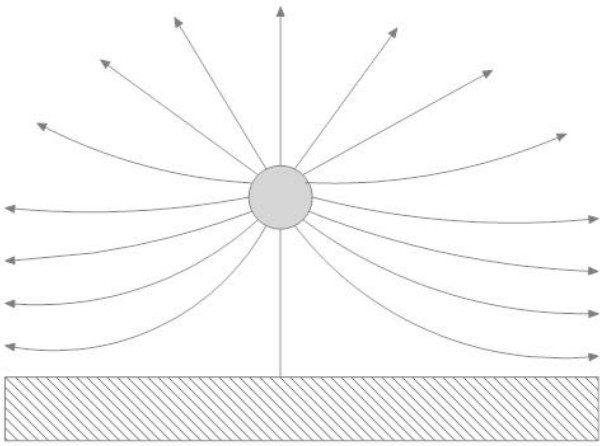

Fig. 3-6 Monopole streamlines near a hard surface.

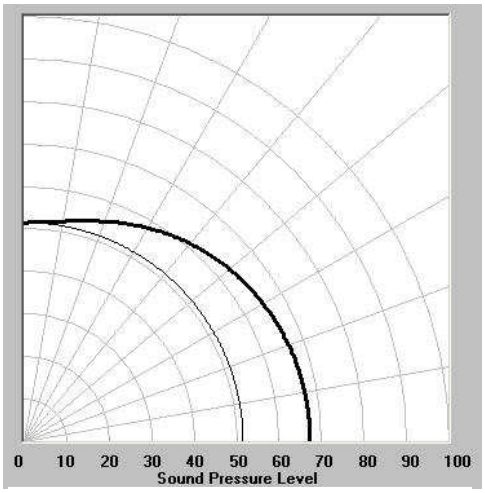

Fig. 3-7. Directivity difference from that of a free monopole.

3.8.3 An Exhaust Pipe in Free Space

Many air handling systems exhaust through a pipe projected high above the ground. The approximate streamlines of the fluctuating mass flow from the pipe are shown in Figure 3-8. The divergence of the streamlines in the opposite direction from the flow is much greater than that along the axis strongly suggesting that the sound pressure along the axis is greater than that in the opposite direction. Measurements of the sound field surrounding a fluctuating mass flow from a pipe are shown in {3.10.4}. They suggest that the streamline approach has limitations (wave diffraction), especially at very low frequencies. When the duct diameter is less than about one-third a wavelength, the estimated

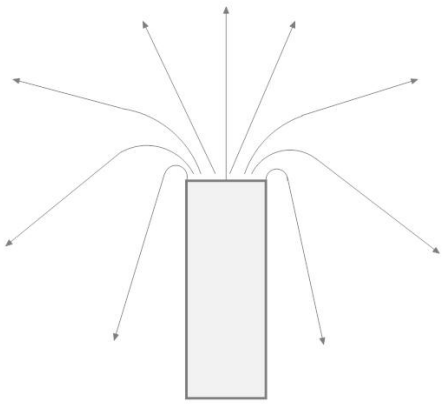

Fig. 3-8. Streamlines near a pipe exhaust.

directivity shown in the figure is erroneous.

An alternative view of the exhaust flow is to consider the development of a ring vortex during the exhaust phase as shown in Figure 3-9. In this view the flow circulation from the vortex development induces a back flow due to the incompressible circulation around the vortex. Some of this mostly incompressible flow has a compressible component in the backward direction.

The model in Figure 3-9 is tied to that in the dipole chapter as an evolution from monopole radiation to dipole radiation {4.x.x}

Key Point: The streamline model for exhaust flow does not predict the sound field at low frequencies.

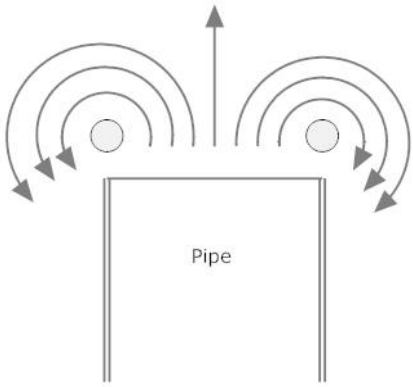

Fig. 3-9. Alternative view of pipe exhaust streamlines.

3.8.4 An Exhaust Pipe near a Reflecting Surface

A typical example of this geometry is the exhaust of an automobile. Figure 3-10 shows approximate streamlines. The sound in the reverse direction is expected to be much weaker, as in {3.8.2}. The stagnation point requires that the flow toward the surface be redirected to the right, causing the streamlines to be closer and so result in higher levels along the surface in the exhaust direction.

Key Point: Although no directivity data were found, it is highly likely that the sound field is a maximum on the ground along the exhaust axis.

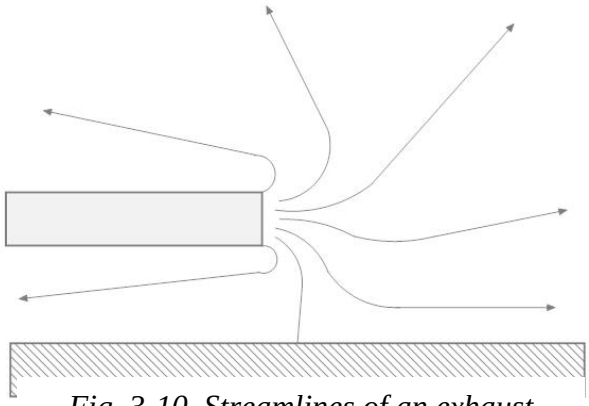

Fig. 3-10. Streamlines of an exhaust flow near a surface.

3.9 Directivity of Monopole-like Sources

One of the tools in identifying the type of sound source, is its directivity. The simple streamline approach above is useful but has limitations for source identification. Below are examples of fluctuating volumetric flows from several objects showing why deviations from monopole sound field uniformity occurs. Since the volumetric flow is not radially symmetric, the sources cannot be classic monopoles; they are called *monopole-like*. Many practical problems relate to the sound emitted from flows exhausting from structures such as pipes. Since the volumetric flow rate is not radially symmetric, neither is the sound field, so the theory cannot be applied with regard to directivity. Several examples of non-uniform volumetric flows are given in this section.

3.9.1 Piston Source in a Plane Surface

A classic model in textbooks is the radiation from a circular piston embedded in a plane surface [6]. It deals with the motion of an infinite solid material at a single frequency. Mathematically, the piston is a distribution of point monopoles over the piston surface (more complex than just two monopoles {3.4}). The equations have been solved. The total volumetric flow fluctuation is the fixed velocity amplitude of the piston times its area. The back reaction of the sound from one point on other points is not considered since the motion is specified. The time delays from various points on the surface result in either reinforcement or cancellation at higher frequencies. Figure 3-11 shows the directional characteristics for three frequencies. In the far field, the level directly above the piston center remains the same (not true in the near field). The lobes at higher frequencies occur as shown. Since the figure is a two-dimensional slice of the actual pattern, the two high frequency lobes are more like donuts. At what frequency can the entire piston be treated as a point monopole with uniform directivity in the hemisphere? The directivity term for the sound pressure in the sound far field for a piston is shown in the first expression on the right. $\mathbf{J_1}$ is the Bessel function of the first kind and order one (F. W. Bessel, 1785-1846). The variable $\boldsymbol{a}$ is the piston radius. Performing a series expansion of the function, and requiring that the second term be only one-tenth the first yields the inequality in the second expression. Below that value, the hemispherical sound field is symmetric; the piston acts like a single frequency finite source, despite the fact that the actual source is distributed over the entire piston face. The radiation resistance increases with the square of the frequency as with the theoretical monopole at these low frequencies. It is interesting to note that at low frequencies, the *acoustical* Strouhal number (0.14) is reasonably close to the *fluid mechanical* Strouhal number for flow over cylinders (0.20).

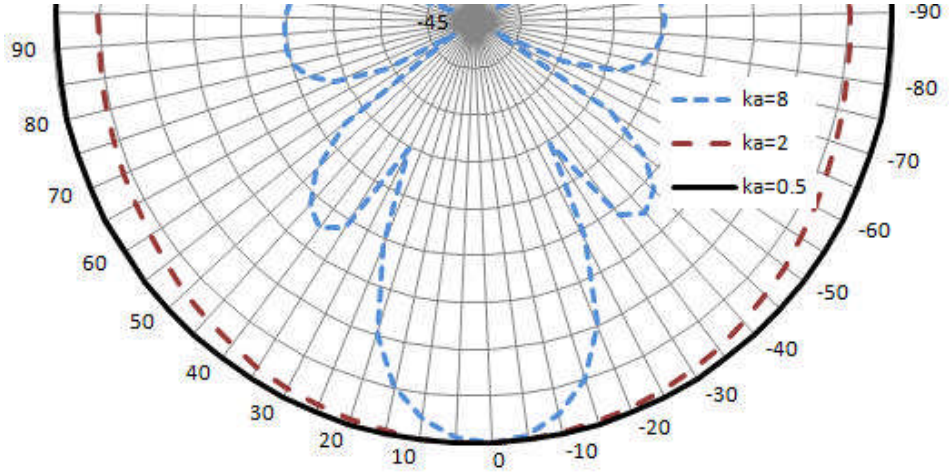

$$\frac{2J_1(ka\sin\theta)}{ka\sin\theta}$$

$$He = ka < 0.89$$

$$St = \frac{fa}{c_0} = 0.14$$

Fig. 3-11. Directivity of a piston source in a plane at three frequencies.

Key Points: If the motion of a surface is coherent and the wavelength is long enough, the distribution of surface sources can be treated as a single source. The characteristic length is the radius of the piston and the characteristic speed is that of piston motion. Note that at low frequencies the hemispherical sound field is nearly uniform despite the fact that the volumetric flow is perpendicular to the surface. Note also that at high frequencies, lobes appear.

3.9.2 Small Piston Source in a Sphere

Another approximation to the theoretical monopole is the sound created by a piston on the surface of a sphere as opposed to that on a plane surface. It deals with the motion of a finite solid material at a single frequency. The theory has been solved [1] and some selected directivity results are shown in Figure 3-12 for a piston that is small with respect to the radius of the sphere. It is interesting to note that constructive interference can occur diametrically opposite the piston position (at 180 degrees), so that a lobe occurs behind the piston. Values of Helmholtz number {A.2.2.2} near 0.5 result in nearly spherical directivity. What happens when the piston radius is larger? The radiation impedance and the directivity pattern changes significantly [1].

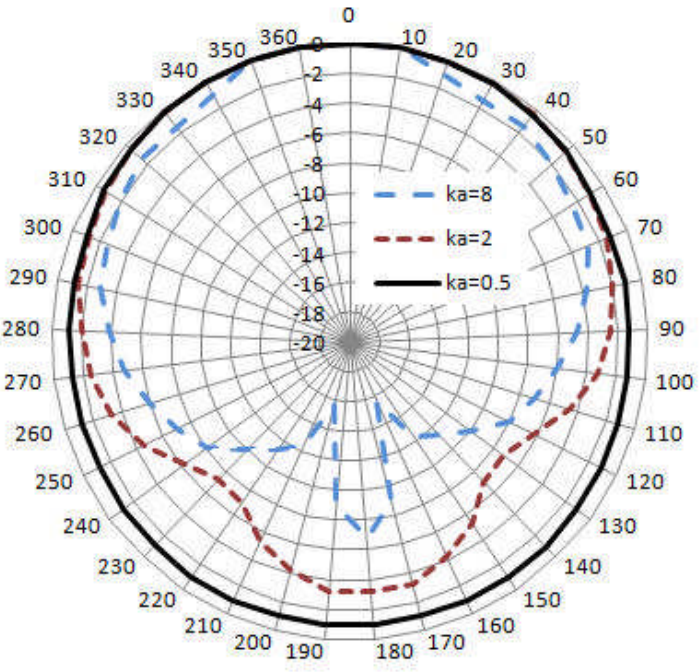

Fig. 3-12. Directivity of a small piston source in a sphere at three frequencies.

Key Points: Fluctuating mass flows from only part of a finite structure create a non-uniform sound field. The directivity is a function of frequency so for a broad-band spectrum, the overall directivity will be determined by the spectrum contour. If the structure is finite and symmetric, it is possible for the level in the opposite direction to be higher than levels at lesser angles. This will not happen for long structures such as exhaust pipes {3.9.4}. For a small piston, the characteristic length is sphere radius and the characteristic speed is that of the piston motion. For a larger piston, there is a second characteristic length, that of piston radius. Note that at low frequencies the sound field is nearly spherically uniform despite the fact that the volumetric flow is perpendicular to the sphere. Note also that at high frequencies, lobes do not appear as readily as with the piston in a plane source. Source geometry plays an important role in directivity.

3.9.3 Loudspeaker in a Cylindrical Cabinet

A loudspeaker placed at the exit and radiating from a cylindrical tube is more like that from an exhaust pipe than that from sphere, except the tube is of finite length (3.2 times the radius in the present example). Here the interest is expanded to a broad-band random noise spectrum from a solid material. There were two spectra, one had a slope of –3 dB/octave and the other had a slope of 0 dB/octave (so-called pink noise). The frequency range was from 100 to 8000 Hz; the Helmholtz number varied from ka=0.11 to ka=9.3. The directivity patterns are shown in Figure 3-13. When the low frequencies dominate, the maximum level difference was 4.7 dB, while for pink noise it was 11.5 dB. Because the length was finite, a small lobe was evident for the pink noise but smaller than that for the spherical source {3.9.2}. The characteristic length is the speaker radius and the characteristic speed is that of the volumetric flow (undetermined for this case).

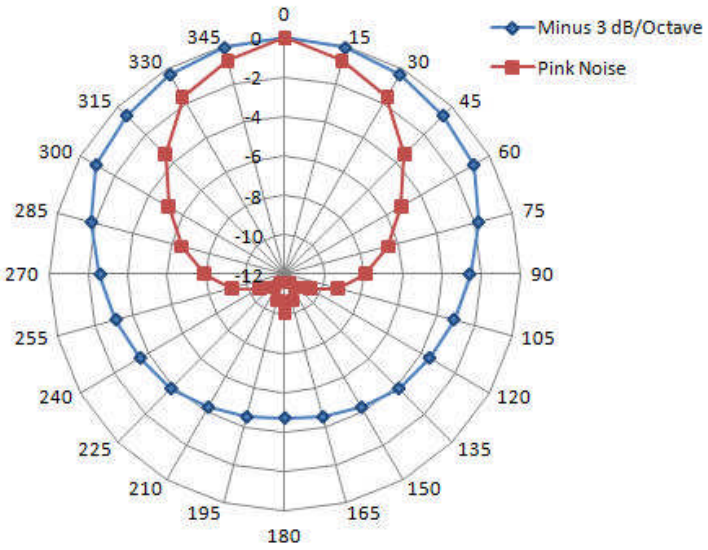

Fig. 3-13. Sound pressure directivity of a cylindrical speaker.

Key Points: The directivity of a broad-band fluctuating volumetric flow depends significantly on the spectrum contour, reducing the usefulness of directivity as a tool for source identification. In many practical situations, the low frequency spectrum dominates so it is often possible to separate a monopole source from that of a dipole, the other common source type.

3.9.4 Exhaust Flow from a Pipe

Several types of sources can be present in the exhaust from a pipe. This example is restricted to a fluctuating volumetric flow at a single frequency. Levine and Schwinger provided a theoretical framework for the sound field from a pipe of semi-infinite length in a free field. Ando [17] made measurements for comparison with the theory. Although the agreement was not exact, it was close. Figure 3-14 shows the measured directivity for three values of the Helmholtz number. The characteristic length was pipe radius. The characteristic speed was that of the exhaust flow.

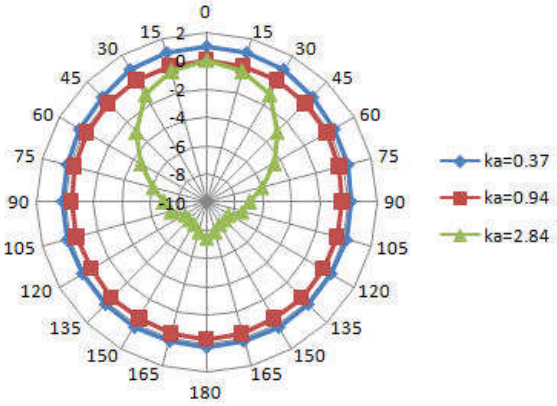

Fig. 3-14. Directivity of cylindrical pipe sound at various frequencies.

Key Points: The directivity of a fluctuating volumetric flow from a pipe differs significantly from that of the theoretical monopole. Sound field non-uniformity is sufficiently small to be neglected if **ka<1** (St<0.16). This conclusion compares favorably with that of {3.9.1 and 3.9.2}, so that for prominent frequencies below this criterion it would be possible to use directional characteristics as a tool to identify a monopole source.

3.10 Modeling Monopole Sources

The basic feature of the theoretical monopole is a spherically symmetric fluctuating volumetric flow rate with a spherically symmetric sound field. Some real sources may meet these requirements such as bubble collapse, balloon pops, or the world's largest monopole: the 50 megaton H-bomb at Novaya Zemlya. In many other cases, the fluctuating volumetric flow is highly directional, as suggested in {3.8, 3.9}, so it should be described only as *monopole-like.* Monopole and monopole-like sources can be grouped based on the physical geometry of th e source:

1. *A symmetric fluctuating volumetric flow rate in free space, such as an explosion.* It creates a sound field that is symmetric and fits well with the theoretical model.
2. *A fluctuating volumetric flow rate caused by the motion of a plane surface, such as a loudspeaker*. The volumetric flow is in one direction only and symmetry of the sound field in half space can be achieved only at low frequencies.
3. *A fluctuating volumetric flow rate from a tube, such as an exhaust pipe.* The volumetric flow is in one direction only and symmetry of the sound field can be achieved only at low frequencies. If the source is a circular tube exhausting gas, the tube can have cross and spinning modes that complicate the radiation process from the opening; the exit plane no longer can be considered as a distribution of in-phase monopoles. These modes can be broad-band or a single frequency. In many of the applications modeled below, it is highly unlikely that significant cross or spinning modes exist to degrade the analysis. Spinning modes are generally associated with gas turbines.
4. *A fluctuating volumetric flow rate from more complex shapes, such as between the treads of a tire in motion*. The volumetric flow rate may be a function of angle creating a more complex sound field.
5. *A fluctuating volumetric flow rate from specifically designed surfaces, such as special loudspeakers.* To enhance the sound level in specific directions, loudspeakers are often designed with complex shapes that modify the directivity of the source.

Note that the above situations apply in a free field and are not related to contributions from reflecting surfaces.

The purpose of modeling in the next sections is not to display clean solutions to actual problems, but rather to show how to put a knowledge framework around specific sound sources by use of scaling rules and dynamic similarity principles with hope that the same technique can be used by the reader for other sound sources.

3.11 Modeling Category I Monopole Sources

Category I sources are those in which the generated sound is primarily a by-product of source motion {1.4.1}. Although most of the mathematical monopole models developed above are approximations to reality, it is still possible to learn much about an actual sound source using the models along with a judicious choice of the characteristic variables.

3.11.1 Combustion

It is beyond the scope of this monograph to develop the details of the sound field created by the reacting fluid motion of combustion. It is clear that the combustion of flammable gases produces a rapid expansion of the gas, but certain types of combustion do not create sound. For example, the Bunsen burner is quiet; the flame speed into the burner flow is balanced by the exiting gas speed so the flame front (density change) is stationary with regard to an observer {2.1.1}. The flow is laminar so there is no time component at the flame front and thus no sound. Here is a case where the density changes but no sound is created. Propane torches are similar, but have a turbulent gas flow. The turbulence creates temporal fluctuations at the flame front and thus sound. Does the collection of monopole sources distributed across the flame front create an overall monopole sound field? Measurements on a propane torch are shown in Figure 3-15. Measurements were made at two positions 90 degrees apart in the plane of the orifice, and at one position 45 degrees to the flow axis, another on the axis and one at 170 degrees from the axis. The monopole nature of the sound field is clear. Despite the fact that the flame front was somewhat shadowed by the structure of the torch, the 170 degree measurement agreed reasonably well with the others and particularly with the on-axis measurement.

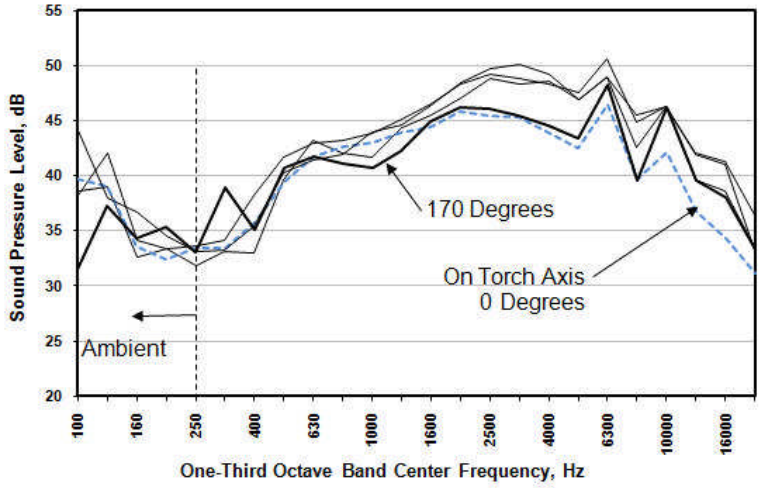

Fig. 3-15. Spectra of a propane torch.

Key Points: The symmetry of the sound field is a strong indication that all of the sources are monopole so the flame is an acoustically compact collection of monopoles distributed along the conical flame front. The source strength is the gas expansion upon combustion. The variables characteristic of the combustion process are not easily available. Here the actual characteristic lengths would be the turbulent eddy sizes proportional to the measurable burner radius. The characteristic speed would be the turbulent eddy speeds proportional to the gas efflux velocity. As a result, the characteristic variables have a spectrum of sizes and speeds resulting in a broad-band spectrum of sound.

3.11.2 Explosions

A typical explosion will create a transient monopole field close to the theoretical, absent of any reflecting surfaces. Chemical explosions come in a variety of forms, some bounded. Weapons discharges can be considered to be transient versions of pipe exhaust flow; they can be subsonic or supersonic. Modern weapon discharges typically are supersonic, so they result in the familiar crack with little subsequent sound. Other materials can combust slowly or proceed to detonation. Typical explosive sound spectra at a distance are shown in the Figure 3-16. As a finite monopole it does not suffer from the flattening of the radiation effectiveness since the frequencies are quite low {6.4.3}. The world's biggest monopole is the hydrogen bomb. It most assuredly does not meet the linear wave equation requirements {2.2.6, D.2}. The initial shock wave is succeeded by massive flows of material which create their own sound as well as creating sound by the passage of powerful winds around structures.

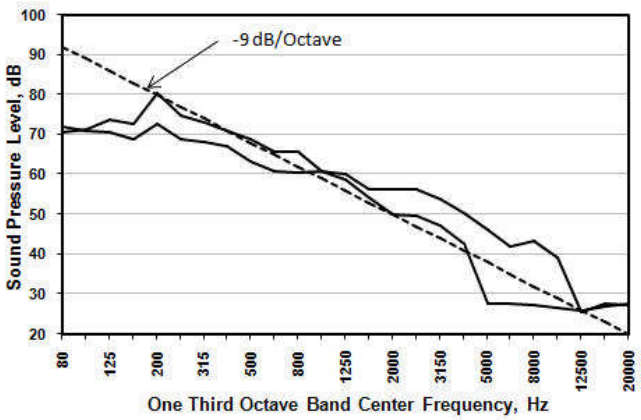

Fig. 3-16. Typical explosion spectra.

Key Points: Free explosions are inherently monopole in nature and the sound wave from them can vary from a shock to a transient sinusoid. The conversion of the stored energy to a gas defines the sound strength. Since this is a transient phenomenon, is knowing the characteristic variables useful or relevant?

3.11.3 Vergeltungswaffe Eins (V1)

This is the first example of converting the fluid mechanics of exhaust flow from a tube to a sound field. The lack of a flange makes mathematical analysis of the sound field more difficult {3.9.4}. As will be seen later, there can be more source types involved in exhaust flow than the fluctuating volumetric flow rate addressed here {6.4.4}. In October 1937, Werner von Braun (1912-1977) and Walter Dornberger (1895-1980) opened a weapons development area at Peenemunde, Germany. One of their weapons, created by Robert Lusser (1889-1969), was called "vengeance weapon one" in Germany, and the "buzz bomb" or "doodle bug" in England. A photograph is shown in Figure 3-17. It was flown from German controlled territory mainly to London. As long as the engine sound existed there was no problem, but when it cut out, the bomb descended. It was powered by repetitive bursts of combustion resulting in a periodic mass outflow that propelled it. The XP90 pulse jet was mounted above the aircraft body. Air entered the front of the jet tube through a louver. Fuel was added and combustion occurred, closing the intake louver and expelling the gases through the tube (about 10 inches in diameter). As pressure in the tube dropped, the louvers opened and the cycle restarted. It is clear that the mass flow into the intake and out of the exhaust would create two monopole-like sound sources, the periodic mass flow rate out of the exhaust greatly exceeding that of the inflow. There are many modern air and land vehicles that are propelled with such a device. Videos had been made of the actual

launch of the V1, probably in Belgium, and the sound spectrum at launch was recorded. A spectrum, at an arbitrary level and at an unknown angle, is shown in the Figure 3.18. Documents suggest that the pulse frequency was between 10 and 100 Hz and the data in the figure suggest it was in the 100 Hz one-third octave band. Although the harmonics show, it is clear that the flow was excessively turbulent. The engine thrust **F** of 600 lb_f was most likely generated during flight but the number is still useful for estimates. The characteristic length is the exhaust diameter, and

Fig. 3-17. Vergeltungswaffe Eins

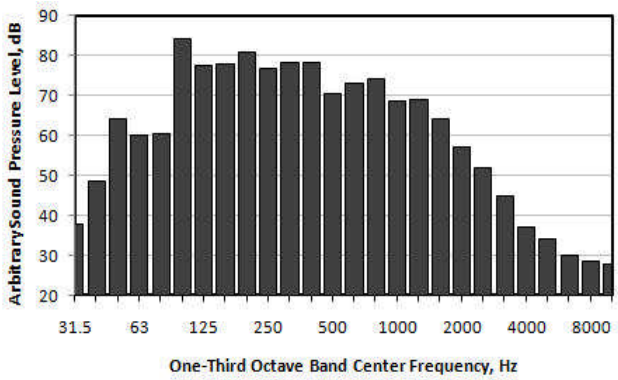

Fig. 3-18. Spectrum of V1.

the characteristic steady speed is the average characteristic speed (exhaust) can be deduced from the thrust. Consider the device to be primarily a momentum machine with the exhaust momentum much larger than the inlet momentum. If the thrust for calculations is considered to be the mean thrust that propels the V1 (as opposed to the peak thrust during the cycle), the mean exhaust speed can be calculated. Since the frequency is low, the point monopole model can be used to make estimates of the sound pressure levels from the device, as shown in Eqs. 3.29. The pulse exists for about half the duty cycle, the half amplitude of the fundamental is about equal to the magnitude of the mean flow during that time. If the density difference between the ambient air and the exhaust gases (an unknown variable) is neglected, calculations yield an estimate for the sound pressure level with distance as shown in Figure 3-19. There is little doubt that this weapon was loud!

$$U = \sqrt{\frac{F}{\rho_0 \pi D^2}}$$
$$Q = U \pi D^2 \qquad (3.29)$$
$$W = \frac{k^2 Z_0 Q^2}{4\pi}$$
$$L_p = 10 * \log_{10}\left[\frac{Z_0 W}{4\pi r_2 p_R^2}\right]$$

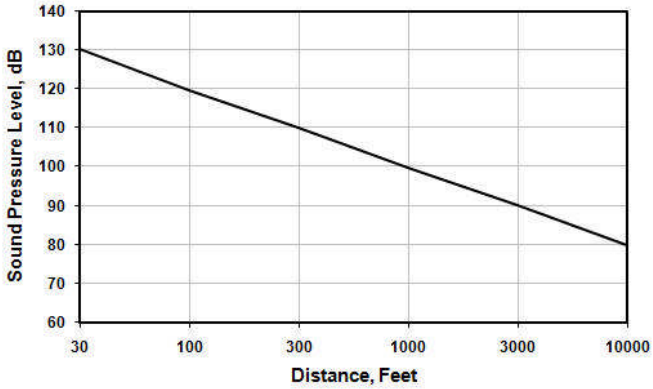

Fig. 3-19 Estimated sound pressure level of V1.

Is the estimated sound pressure level accurate? No, this result applies only for the pulse frequency. Is it in the "ball park"? Yes, the remainder of the spectrum will add somewhat to the overall level. The estimate was based only on knowledge of the pulse frequency, the exhaust diameter, and the engine thrust; data which are seldom used for acoustical purposes.

Measurements of V1 sound pressure level directivity have been made and the averages are shown in Figure 3-20. The direction of flow is toward the 0 angle (exhaust) and the level on the intake axis is about 11 dB down from the exhaust axis. This figure includes all frequency components. This results shows that the intake monopole is relatively weak. The directivity results of Figure 3-20 compare well with those from Figure 3-13 for the cylindrical loudspeaker with pink noise; the higher frequencies contribute significantly to directivity.

Key Points: Knowing the characteristic variables and the nature of the sound source, it is possible to make a rough estimate of sound pressure levels based on some known mechanical variables.

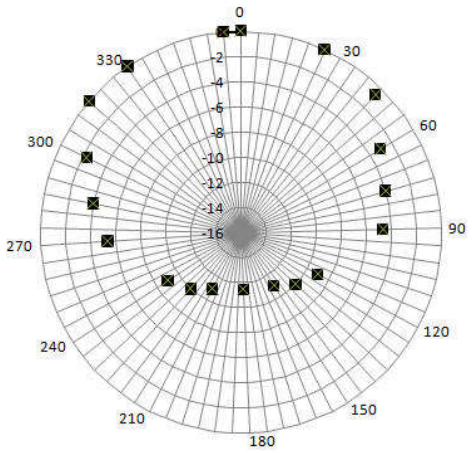

Fig. 3-20. Directivity of V1 sound.

3.11.4 The Vibrating Rectangular Membrane

Instead of a piston source, consider a membrane vibrating in a plane. Morse included such an analysis in his classic book [2]. The pertinent relations are

$$z_{mn} = A\sin\left(\frac{\pi m x}{a}\right)\sin\left(\frac{\pi n y}{b}\right)\cos(\omega_{mn} t)$$
$$\omega_{mn} = \pi\sqrt{\frac{T}{\sigma}}\sqrt{\left(\frac{m}{a}\right)^2 + \left(\frac{n}{b}\right)^2} \qquad (3.30)$$

The vertical displacement $\mathbf{z_{mn}}$ is given for any position (**x** and **y**) of any (**m** and **n**) mode number in a rectangular membrane of dimensions **a** and **b**. The wave speed is determined by the membrane tension per unit length **T** and the mass density **σ** per unit of area of the membrane. The frequency **ω** and the wave number **k** is determined by the wave speed and the mode shapes. For example, the **m=n=1** mode is the drum mode with the center of the membrane being the maximum displacement point (upper left of Figure 3-21). The **m=n=2** mode results in four areas of motion. Two of the diagonally opposite areas are in phase, while the other areas are in phase opposition (lower right of Figure 3-21).

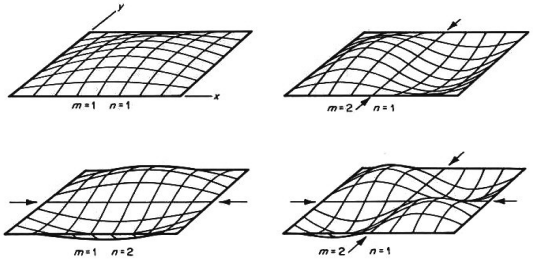

Fig. 3-21. Lower mode shapes of a vibrating membrane.

But what about the sound radiated from this motion? To integrate the contribution from each position on the membrane is a formidable task. It is clear from the figure that each mode area causes a volumetric displacement of the surrounding medium and the phase of the next mode is opposite.

If each mode area within a rectangular array is considered to be a monopole source the sound field velocity potential can be written as

$$\phi = \frac{Q}{\pi} e^{i\omega t} \sum_{a=1}^{m} \sum_{b=1}^{n} \frac{e^{-i(kr_{ab}+\delta_{ab})}}{r_{ab}} \tag{3.31}$$

The source strength can be determined by integrating the displacement over a particular mode area to get **Q=4A** where **A** is the r.m.s. amplitude of each mode shape. Since the total membrane area may be large, the far geometric field assumption is not used; the distance $\mathbf{r_{ab}}$ is that from the mode center to the measurement point. The phase term **δ** is either **0** or **π** for alternate source positions. The equation for the mean square pressure is

$$\mathrm{Re}\left[pp^{*} \right] = \frac{k^2 Z_0^2 Q^2}{16\pi^2} \left[\sum_{a=1}^{m} \sum_{b=1}^{n} \sum_{c=1}^{m} \sum_{d=1}^{n} \frac{\cos\left[k\left(r_{cd} - r_{ab} \right) + \left(\delta_{cd} - \delta_{ab} \right) \right]}{r_{ab} r_{cd}} \right] \tag{3.32}$$

Note that the volumetric flow rate in each mode area is assumed to be the same, although it may be different for different sets of modes. Replacing the integrals with summations must be based on the assumption that the wavelength is long with respect to the mode length; each mode area radiates as if it were a monopole. Summations lend themselves to computer modeling, and this has been done in **SoundSource**.

This situation is like several rectangular shaped pistons embedded in a plane. If the criterion used for the piston is applicable, the criterion for each mode to radiate as a point monopole is

$$St = \frac{fL}{c_0} = 0.28 = \frac{c_m}{c_0} \sqrt{\left(\frac{mL}{2a} \right)^2 + \left(\frac{nL}{2b} \right)^2} \tag{3.33}$$

L is the lesser of the two dimensions and the membrane wave speed is $\mathbf{c_m}$. Therefore, the point monopole model would be applicable at low membrane wave speeds relative to the sound speed and at low mode numbers. The same concepts can be applied to circular membranes but Bessel functions are needed in the development.

Key Points: In many realistic situations, the correct but difficult integral formulation can be replaced by a summation that can be computed readily. There are two characteristic lengths, the smaller of which is the critical one. The characteristic speed is the wave speed of the membrane vibrations that define the frequency.

3.11.5 The Harley-Davidson Motorcycle

Owners of these motorcycles seem to love the sound created, particularly during acceleration, so the bikes often have straight pipes. If these owners bike to a rock festival, their cochlea will have a very bad day. The primary source is likely to be monopole-like above a reflecting plane due to the periodic exhaust flow {3.4.3, 3.9.4}. Figure 3-22 shows a passby spectrum as measured at 18 feet; the speed was close to 45 mph. The maximum of 103.2 dB occurred in the 125 Hz one-third octave band, but it is clear that the exhaust flow was very turbulent resulting in a broad-band spectrum. For comparison, Figure 3-23 shows the passby spectrum of a quieter motorcycle under the same conditions. The maximum of 75.4 dB occurred in the 125 Hz band. Note the lack of severe turbulent flow noise. Since the wavelength was much greater than the exhaust radius, the point monopole version of Eq. 3.20 was used to

calculate the approximate sound power so hemispherical uniformity is likely, except for the reflective influence of the motorcycle body. Taking into account the hard reflection, the sound power and rms volumetric flow rate was using the equations below. For the Harley the overall sound power was estimated to be 12 Watts for the Harley and 0.01 Watts for the quiet motorcycle; an impressive difference. The oscillatory volumetric flow rate that resulted in the sound was estimated for the Harley to be 3.7 ft^3/sec while that for the quiet vehicle was 0.22 ft^3/sec; a significant difference.

The contribution of tire noise (see Figure 3-24) near 1000 Hz shows in both the spectra.

These concepts can be applied to the exhaust of racing vehicles as well. The author measured the sound of Indianapolis race cars when both reciprocating and gas turbine engines were permitted. The turbines were so quiet they were booed by the race crowd, despite the fact that they were faster. They were banned. Which was the more important criterion for racing vehicles; speed or noise?

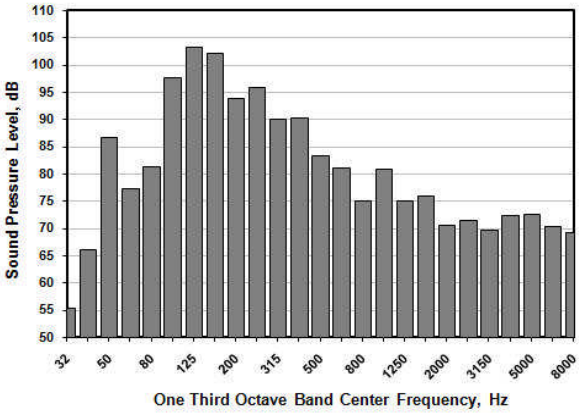

Fig.3-22. Frequency spectrum of Harley-Davidson motorcycle sound.

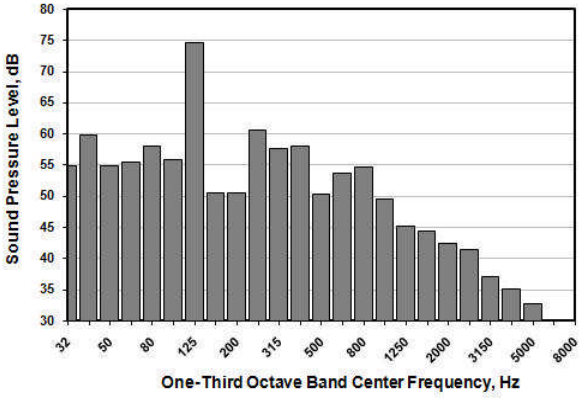

Fig. 3-23. Frequency spectrum of quiet motorcycle.

Key Points: To properly calculate the sound power of a vehicle exhaust, the sound pressure must be integrated over the hemisphere surrounding the source, which is only possible with the vehicle standing still and running on a drum in a proper environment. To calculate from a passby, the monopole surface reflection {3.4.3} must be taken into account, but the directivity model, which is based on the spectrum contour, is more difficult. The results in {3.9.4} may be useful. With these defined, the monopole model may be used to derive reasonable estimates of sound. Good mufflers make good neighbors (apologies to Robert Frost). When the exhaust flow fluctuation is predominantly one frequency, it is possible to estimate volumetric flow rates and exhaust velocities. The characteristic length is the exhaust diameter. The characteristic speed is that of the exhaust, but that is difficult to determine, so the vehicle speed must be used. It is likely that one is proportional to the other.

$$W = \pi r^2 \frac{p_R^2}{Z_0} 10^{\frac{L_p}{10}}$$

$$Q = \sqrt{\frac{4\pi W}{k^2 Z_0}} \qquad (3.34)$$

3.11.6 Automobile Tire Sound

This is an example of a complex source generation situation that has had considerable study. There are a number of actual sources on an automobile, but modern design has reduced all but the noise from tires (except for certain vehicles with predominant exhaust noise). Years ago there was a question about the nature of the sound from tires. Was it casing or tread noise? Figure 3-24 shows a typical one-third octave band sound spectrum of a "quiet" automobile moving at about 45 mph. The frequency at the maximum is in the 1000 Hz one-third octave band. The mass continuity equation suggests that the Strouhal number be of order one, so using Strouhal modeling, with $0.1<St<1$, the characteristic length **L** is found to be between one-sixteenth inch and three quarters of an inch. This result strongly suggests that the source is not the casing. The low frequency maximum in the spectrum, near 63 Hz, is likely related to engine RPM and therefore to exhaust noise {3.11.5}. From this modeling, it seems clear that the characteristic length is *tread size* and the characteristic speed is *vehicle speed*. The spectrum for a large pickup truck has a maximum in the 800 Hz band at similar speeds, reinforcing the tread as the characteristic length since it has larger and deeper treads.

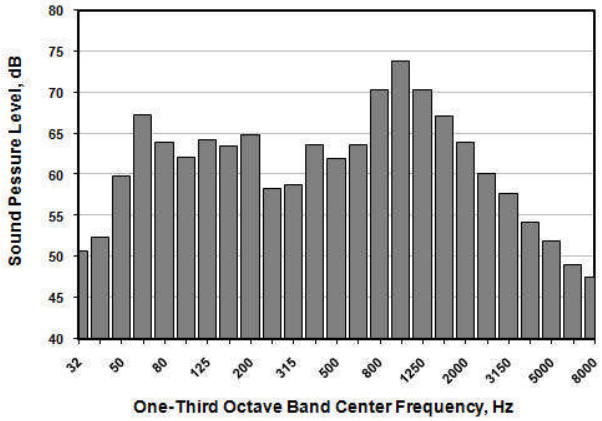

Fig.3-24. Frequency spectrum of passenger automobile sound.

What happens to the treads? Recent research [18] has suggested that there are four mechanisms for tire noise: air pumping, tread block motion, tread contact, and tread separation.

Air pumping is compression of the air between treads; the treads must be compressed and distorted when encountering the road surface. Some of that action results in compression of the air between the treads which should result in monopole-like sources. The level of the sources should be a *maximum lateral* to the vehicle direction. Tread block motion is the deformation of the tread bodies themselves while in contact with the pavement. This is likely a dipole source if the correlation between them is substantial {4.9.6}. Tread contact and separation occurs as the treads first contact the road and then leave it. These events must be monopole-like, but out-of-phase, so may be like two nearby monopoles that act like dipoles at low frequency. Their levels should be a *maximum in the direction* of vehicle motion. The shearing of the tread block should result in quadrupole sources, but the relative inefficiency of these latter sources {5.1} suggests that their contribution is small. Road roughness adds to the source strength for each of the above mechanisms. Figure 3-25 [19] shows the speed dependence of tire

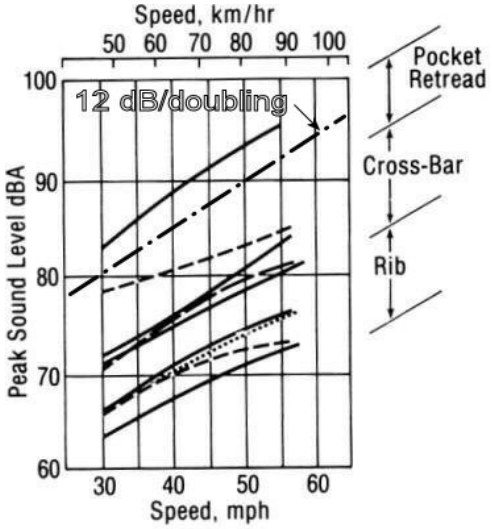

Fig. 3-25. Speed dependence of tire noise.

noise from both trucks and automobiles. The data compare very favorably with the U^4 law of {3.2.8}; a 12 dB increase per doubling of speed.

Figure 3-26 [18] shows a more comprehensive set of data for the speed dependence of automobiles and trucks and for a variety of road conditions and measurement methods. The heavy line is the monopole speed dependence. The scatter in the data makes the mean lines unreliable for exact comparison, but the trends are clearly more like a monopole source than that of a dipole (18 dB per doubling of speed). Trucks with larger treads create more "pumping" sound (volumetric flow rate fluctuations) and fit the monopole model reasonably closely. A local test was performed. One automobile was driven by at two speeds; 30 and 60 mph over the same road. The maximum passby spectra were measured. The dynamic similarity equation (Eq. 3.10) was used to adjust the high speed data in both level (U correction) and frequency (Strouhal correction). The two spectra are shown in Figure 3-27. The close match of the adjusted high speed data to the low speed data at the maximum strongly supports the monopole nature of the source and thus tread air pumping as the predominant sound source. The spectrum slope above the maximum for these two samples do not agree closely, suggesting that the source strength term in Eq. 3.10 may be speed (Reynolds number) dependent at higher frequencies. It is interesting to note that the spectrum slope above the maximum level (for much of the data taken) very closely followed the -9 dB/octave slope (f^{-3} dependence) as was found for several other sources.

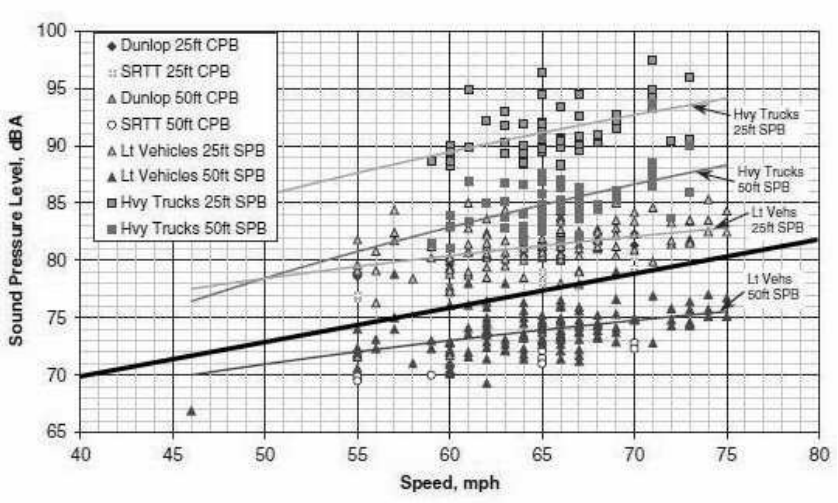

Fig. 3-26. Data on various vehicles, tires, and road surfaces. Heavy line is U^4.

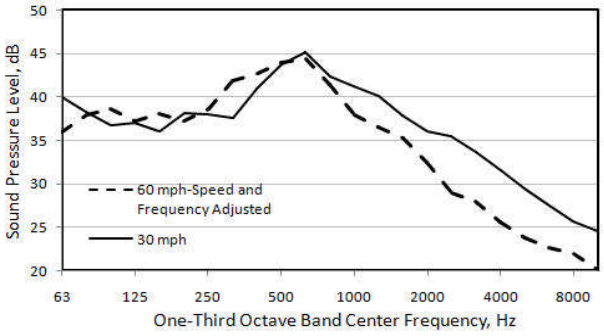

Fig. 3-27. Comparison of two passby spectra of an automobile with one spectrum corrected for level and spectrum.

Key Points: Strouhal modeling was used to define the characteristic length (source size). The speed dependence was used to define the source type and the characteristic speed; vehicle speed. To reduce tire noise based on the monopole model, the motion (distortion, compression) of the treads must be such as to minimize the mean square of the rate of volumetric flow, or mass flow, rate between the treads.

$$I_m(r) = \frac{Z_0}{16\pi^2 r^2 c_0^2}\overline{\left(\frac{\partial Q_m}{\partial t}\right)^2} = \frac{1}{16\pi^2 r^2 Z_0}\overline{\left(\frac{\partial M}{\partial t}\right)^2}$$

There are two monopole configurations. The first is air pumping perpendicular to the direction of travel; it is likely to have a maximum level in that direction. The second is the contact/separation event; it is likely composed of two monopole-like sources out-of phase and with a maximum level likely to be in the direction of travel. Separation of these types might be done by measurement of treadless tires such as those used in race cars.

3.11.7 Bubble Formation/Collapse

The formation or collapse of a bubble should represent a transient monopole in a relatively free field. High speed data on bubbles in water suggest very high collapse rates and large expansion wave pressures, so bubble collapse can create significant sound. Submariners have always been concerned about propeller cavitation noise so there has been considerable study of bubble collapse. If bubble size is used as the characteristic length, and the collapse rate as the characteristic speed, it would suggest that bubble frequencies are predominantly at high frequencies. However, bubble size is not always constrained to be small. Any form of cavitation or boiling will result in a broad-band spectrum. Boiling water in open pots, for example, has been known to create almost pink noise. The spectrum is the result of a distribution of bubble sizes and formation/collapse rates. It is likely that in a free field the overall directivity of all bubble motion will be close to the classic monopole, similar to {3.11.1}

Key Points: Bubbles are inherently monopole sound sources. The characteristic length is maximum bubble diameter and the characteristic speed is the rate of formation or collapse. These characteristic variables should be used in any research; they will have a distribution that defines a sound spectrum.

3.11.8 Splashes

The sound of liquid droplets falling on a surface depends importantly on the character of the surface. If the surface is a large, stiff and massive (highly inelastic) solid, any sound created is due solely to fluid motion. If the surface is an elastic solid, such as a thin metal plate, the spectrum of the sound depends critically on the mode of vibration excited by the drop. If the surface is a fluid, not only are surface waves created but the possibility of bubble formation\collapse occurs. As with bubbles, the characteristic length is droplet diameter and the characteristic speed is that of each droplet. For one drop, the spectrum is well defined and the radiation should be monopole-like {3.9.1}. Multiple droplets are addressed in {3.11.9}.

One technique to reduce splash noise is the introduction of a screen to break droplets into very small droplets. The technique reduces the characteristic length (droplet size) and the characteristic speed (droplet speed) and thus shifting both frequency and sound level. It is used to quiet home washing machines, and was the subject of a 19th century US patent where the lifting of a toilet cover deployed a screen across the toilet.

Key Points: The sound from liquid splashes on liquid surfaces can be interpreted as a monopole-like sources located at the surface. The characteristic length is droplet size and the characteristic speed is droplet speed. Multiple droplets create a spectrum of characteristic variables.

3.11.9 Waterfall Noise

Waterfalls are examples of complex sound sources based on splashes. Typically, the sound results from both bubble formation\collapse {3.11.7} and droplet impact {3.11.8}. A waterfall is a massive collection of droplets falling on an already disturbed water surface. Consider the impact process. Some waterfalls start with laminar flow, others are already turbulent. The characteristic length (droplet size) and characteristic speed upon impact will depend on the nature of the initial flow; the height of fall and the point at which flow transitions to turbulence. Figure 3-28 shows the sound spectrum of a fifty foot wide waterfall with a fourteen foot drop measured at a distance of fifty feet. The starting flow was turbulent. Significant sound occurs at *very* high frequencies and the spectrum is very similar to white noise (the low frequency deviation of the data is associated with local road traffic noise). Free fall (no drag) estimates give a maximum impact speed near 30 ft/sec for a droplet. It is likely that air drag of droplets is strongly diminished due to air entrainment by the large number of droplets, so that number might not be too high as a characteristic speed. Droplets were on the order of 0.1 inches. Using a Strouhal number range from 0.1 to 1, the spectrum maximum should be between 360 and 3600 Hz. Obviously, there is more to waterfall noise than simple impact. Bubble formation and collapse is the other plausible possibility {3.11.7}. Further, waterfalls have linear extent, so the sound field will depend on the lineal correlation of the various droplets. Falls that remain laminar for a large percentage of the fall will likely decay with distance more like a line source, while larger, turbulent falls will decay more as a linear collection of independent sources.

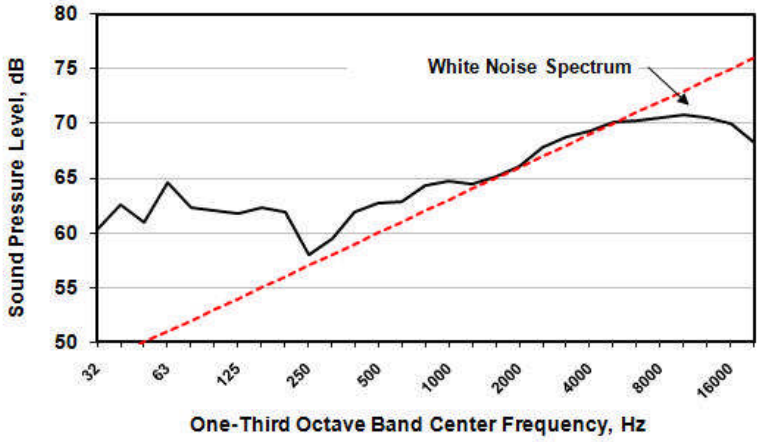

Fig. 3-28. Sound spectrum of a waterfall.

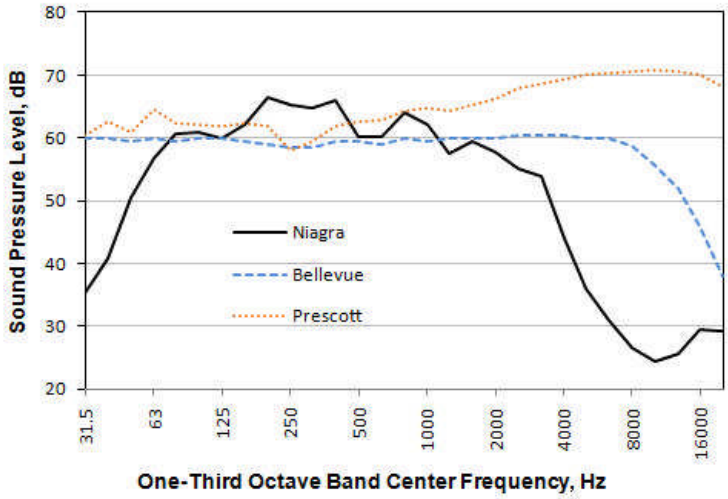

Fig. 3-29. Various waterfall spectra.

Lilly [20] has measured the sound from a waterfall in Bellevue, Washington Park, 200 feet wide and with a 9 foot drop and apparently starting with laminar flow (Figure 3-29). At a measurement distance of 12 feet, the spectrum had a 1 dB/octave slope up to 8000 Hz (nearly pink). This result suggests the characteristic length was larger, and the lack of very high

frequencies suggests that the impact process of the lower fall distance reduced the severity of bubble formation. A number of sound spectra of Niagara Falls at similar distances were taken from a videos and averaged and added to Figure 3-29. The levels were arbitrarily adjusted to fit so the spectral contours could be compared. At the present time there are insufficient data to scale waterfall spectra.

Key Points: Although it is clear that droplet size is the characteristic length and droplet speed is the characteristic speed, the spectra of neither are readily available. The interaction of the splash adds additional complexity to waterfall noise.

3.11.10 Electrical Discharges

All electrical discharges result in rapid temperature and density changes that propagate as sound. Sparks are monopole sources while corona discharges may be line sources. Electrical discharges are not covered in this monograph

3.12 Modeling Category II Monopole Sources

Category II sources are those in which the generated sound has a strong impact on the source that creates the sound {1.5.2}. Again, it is still possible to learn much about a sound source using the monopole models along with the scaling rules and judicious choice of the characteristic variables.

3.12.1 The Hole Tone (Tea Pot Whistle)

The steady flow from a circular orifice can be converted to an oscillatory flow by adding a downstream plate with a circular hole aligned with the orifice. Small perturbations in the flow are fed back to the orifice to cause a variable volumetric flow rate through the hole because of the symmetry of the feedback. The disturbance is amplified along the jet {1.5} forming the feedback loop when the disturbance encounters the hole. Figure 3-30 shows a schematic of the geometry. The oscillatory volumetric flow through the plate hole creates a nearly pure tone monopole-like sound field. This phenomenon is one of many that have been called *aerodynamic whistles*. The frequency depends on the steady flow rate from the primary orifice and is subject to jumps as the phase relationship of the feedback changes. One part of the feedback loop is the incompressible disturbance wave carried with the steady flow from orifice to plate. Since the gap between plate and orifice is typically a small fraction of an acoustical wave length, the other part of the feedback loop is the hydrodynamic field of the monopole source. In a study [21], the characteristic speed was chosen to be the average speed of the jet at the orifice (deduced from measured volumetric flow rate). The characteristic length was chosen to be the orifice diameter. Figure 3-31 shows the Strouhal

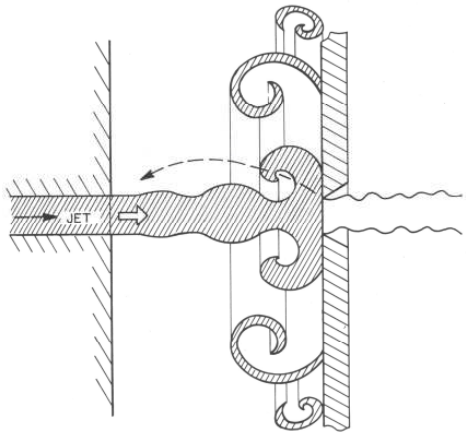

Fig. 3-30. Hole tone geometry.

number as a function of the Reynolds number based in these dimensions. The hole and orifice diameter **δ** for this figure was 5 mm, and **h** was the separation distance between plates, in mm. The use of Strouhal number showed most clearly the almost linear relation between frequency and speed. The nonlinearity of the feedback system is exemplified by the hysteresis loops for each gap ratio.

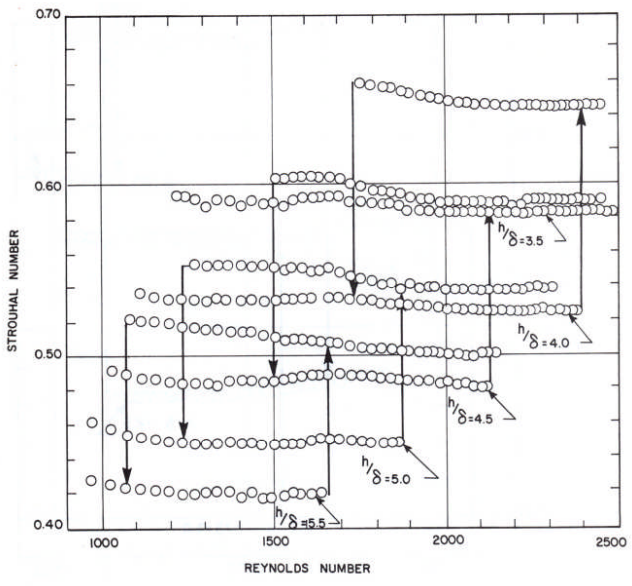

Fig. 3-31. The hole tone frequency

More would have been learned had the characteristic variables been chosen so the hysteresis loops overlapped. The frequency is determined by the plate separation **h** and the wave speed in the jet, which is a fraction of the exit speed. Similarly, the source strength is determined by the oscillatory flow rate at the plate hole. The area of the hole is equal to the orifice diameter **δ** and the flow speed through the hole is a fraction of the orifice speed. There are now two characteristic lengths, **δ** and **h**, and two characteristic speeds. **αU** and **βU**. The variable **α** is the ratio of the jet wave speed to the orifice speed; it must be tied to the spreading of the jet and so must be a function of **h**, the separation distance. The variable **β** is the ratio of the mean speed at the hole to the orifice speed also a function of **h**. These characteristic variables can be entered into the dimensionless sound power equation of Eq. 3.10 to yield Eqs. 3.35. By adjusting the vertical height of the data, a reasonable value of **α** can be determined. By adjusting the horizontal value of the data, a reasonable value of **β** can be determined. The best fit is when the hysteresis loops nearly coincide. When this is done there is a considerably better overlap of the data, from which any deviations from dynamic similarity can be determined.

$$W = \frac{\rho_0 \pi \alpha^2 \beta^2}{c_0} \hat{Q}^2 St^2 U^4 \left(\frac{A}{h}\right)^2$$

$$St = \frac{fh}{\alpha U}, \hat{Q} = \frac{Q_m}{\beta U A}, A = \frac{\pi \delta^2}{4}$$

$$\mathrm{Re} = \frac{\beta U h}{\upsilon} \qquad (3.35)$$

The uniformity of the measured sound field for this source confirmed the monopole-like nature of the source; more correctly it is more like a piston source in a plane {3.9.1}. Measurements of speed dependence showed it to be very close to $\mathbf{U^4}$, further confirming the monopole nature of the source. Because feedback controlled the sound output, the measurements of speed dependence could only be made in the regions of stability between jumps. At higher Reynolds numbers, the flow became chaotic resulting in broad-band sound. Rayleigh (J.W. Strutt, 1842-1919) was aware of the hole tone phenomenon; it was called the *bird cal*" then.

Key Points: This is a case of examining the physics of the situation to arrive at lengths and speeds that are more characteristic of the sound generation process than average values, such as jet exit speed. By adjustment of measurement results, otherwise arbitrary ratios can be determined to provide more insight into the phenomenon. Both the directivity and speed dependence indicate the monopole nature of the source and so permit a dynamic similarity

equation (Eq. 3-35) to be developed. Although this phenomenon occurs at low Reynolds numbers, there seems to be some evidence that a similar event occurs on aircraft landing gear covers with holes and spinning disks with holes.

3.12.2 Hartmann Whistle (Stem Jet)

The previous example was relevant to low speeds, this example pertains to supersonic speeds. When a subsonic jet impinges on a cavity, jet instability becomes part of the feedback loop. When a supersonic jet impinges on a cavity, shock wave instability becomes part of the feedback loop. The *Hartmann whistle* (Figure 3-32) is one example of the latter case. A cylindrical cavity with one end open and facing the supersonic circular jet will result in extremely intense sound. The shapes in the figure represent the shock/expansion cells within the jet. A related configuration, called the *stem jet*, has a central rod in the jet runs through and that supports the cavity. There are a number of other geometric variations, allof which operate in similar fashion. These devices have been studied [22] and reviewed Raman [23]. Here we look primarily at the Hartmann whistle.

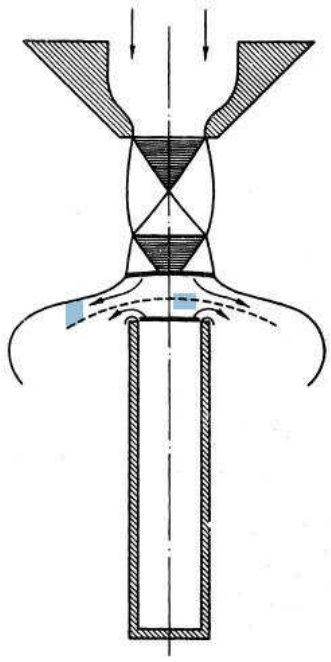

Fig. 3-32 Hartmann whistle.

The shock cells of the jet interact with the shock in front of the cavity (the flow in the cavity being subsonic). Small symmetric disturbances in the jet stream are amplified as they proceed toward the cavity (similar in some respects to the hole tone) causing the shock in front of the cavity to oscillate. The shock front acts much like a piston source of high energy resulting in a monopole-like sound field. Again the volumetric flow is unidirectional unlike the theoretical monopole. The sound field may be similar to that created by oscillatory flow from a pipe, except for presence of the supersonic jet structure which can strongly modify the directivity. The original equation of Hartmann (1881-1951) [24] is the first of Eqs. 3.36.

$$\frac{\lambda}{d} = 5.8 + 2.5\left\{\frac{h}{d} - \left(1 + 0.041\left(P - 0.9\right)^2\right)\right\}$$
$$St = \frac{fd}{c_0} = 0.17 \approx \frac{fh}{U} \qquad (3.36)$$

The diameter of the orifice and cavity being **d**, the distance between orifice and cavity being **h**, and the orifice pressure **P** was given in kg/m^2. At the lower limit of **h** the second term disappears. In this case, the equation could have been reformatted in terms of a Strouhal number as shown in the second equation of Eqs. 3.36. The characteristic speed is shown as that of sound (which is also **U** at the nozzle exit). It is interesting that the number is very close to that found by Strouhal for flow over a cylinder {4.10.1.1}. There are two characteristic length scales. Nozzle diameter **d** characterizes the sound power while the separation distance **h** characterizes the frequency.

Comprehensive studies of this phenomenon [24-26] have shown that the position of the cavity is critical in creating sound. The process has hysteresis loops and the frequencies are related to multiples of the quarter wavelength resonance of the cavity. Reference 23 has a comprehensive discussion of the phenomenon and is recommended for those interested in the physics of the process and the applications of the whistle.

After reformatting Hartmann's formula (the first of Eqs. 3.36), and using Eq. 3.10, we get Eqs. 3.37 for sound power. Since the characteristic speed **U** and $\mathbf{c_0}$ are essentially the same, it can be expressed as the second equation. Although the amplitude factor **A** replaces the dimensionless volumetric flow rate in these equations, the speed dependence strongly confirms the monopole-like characteristics of the Hartmann whistle.

$$W_h = \frac{\rho}{2}\frac{\pi d^2}{4}\left(2\pi\, fa\right)^2 c_0 = A\rho\, f^2 d^2 h^2 c_0 = A\frac{\rho}{c_0}\left(\frac{fd}{c_0}\right)^2 c_0^4 a^2 \qquad (3.37)$$

$$W_h = A\frac{\rho_0}{c_0} St^2 U^4 L^2$$

A cousin to the Hartmann whistle is shown in Figure 3-33; it is called the *Galton whistle.* Here the cavity is excited by an annular jet which oscillates symmetrically around the sharp edges of the cavity. It appears to be a circular version of the edge tone {4.10.5} which is a dipole source. Since it is highly likely that the oscillations are coherent around the periphery, there should be a fluctuating volumetric flow rate from the cavity with only a small net lateral force. Thus the source is yet another version of a monopole-like geometry; the volumetric flow rate is a cylindrical area between the jet and cavity.

Key Points: As with the earlier examples, it is possible to determine the characteristic variables to provide valuable insight about a sound source. For complex phenomenon such as these whistles, such insight is insufficient to lay bare the detailed workings of the mechanism and leads only to suggestions on which variables are important for future research.

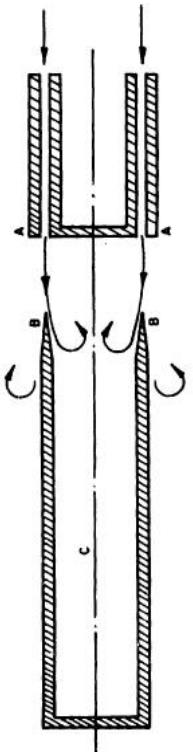

Fig. 3-33. Galton Whistle.

3.12.3 Corrugated Pipe Tone

Pipes with sinusoidal variations of radius are used to permit bending. Steady flow through the pipe at low Reynolds Numbers results in a fluctuating volumetric flow rate that generates a monopole-like sound field at the pipe exit {3.9.4}. Examples of such pipes are shown in Figure 3-35. The plastic pipe is actually a child's toy that sounds when the pipe is whirled around. The metal pipe shown was actually used in the Concorde to provide cooling air to the pilots. It was supplied to the author by John Ffowcs-Williams. The tone was unacceptably loud to the pilots, so it was replaced with a straight cylinder.

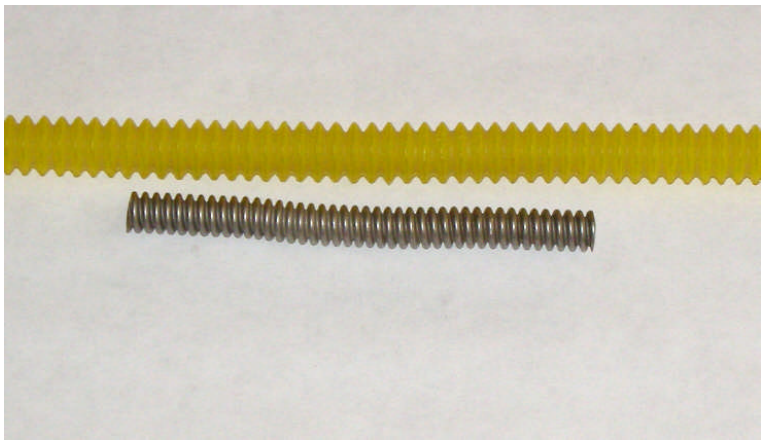

Fig. 3-34. Flow in corrugated pipes can create single frequency tones.

It is similar to the hole tone in that it is due to a periodic volumetric flow rate; is subject to frequency jumps and hysteresis loops but the feedback is internal. The characteristic speed is the mean flow through the pipe and the characteristic length must be a multiple of the spacing between corrugations. Although there is no evidence that this device has been studied in detail, it is likely that the flow instability, being weaker at low speeds, needs to travel several corrugations to establish the feedback loop. As the speed increases, the loop can be established with fewer corrugations.

Simple tests were performed on the yellow plastic tube. The corrugations were 0.011 feet apart. Without knowledge of the Strouhal number or flow rate, the similarity relationship $StU = f_n nL$ was used to determine the number of relevant corrugations. **L** is the corrugation spacing and **n** is an integer. The highest frequency (7554 Hz) was found in the "overblown" condition and **n** was presumed as one corrugation. At the least flow rate, the frequency of 2452 Hz compared favorably to **n=3**. At intermediate flow rates, several non-harmonically related frequencies occurred simultaneously suggesting that several corrugations were involved in the sound generation. In the smaller metal tube, a predominant tone appeared at 6174 Hz and corresponded to **n=2**.

Key Points: The characteristic length for this device is now **nL**, where **n** is close to an integer and **L** is corrugation spacing. Similar to the hole tone analysis, the characteristic speed is that of the disturbance which is likely a fraction of the mean speed through the tube. A unique aspect of this sound source is that the flow carries both the wave amplification and the feedback signal internally. More needs to learned about this device.

3.12.4 Pipe Tone (Pfeifenton)

A cylindrical cavity with a small circular, square-edged hole at one end and totally open at the other is known to generate a tone when air is passed through it. It is subject to frequency jumps and hysteresis loops similar to the hole tone {3.12.1}. The unique feature of this device is that the tone sounds only with flow into the cavity; it is an acoustical diode. It can be blown from the orifice side or suction can be applied from the open end. The fundamental tone occurs near **λ=4L**, so one characteristic length **L** is that of the tube. The characteristic speed **U** is that of the flow through the hole. A monopole-like sound field is generated by motion at either the small or larger end, depending on which end is open. Karthik [27] and Anderson [28] have studied this phenomenon and concluded that symmetric vortex shedding on the cavity side is the driving agency. An example of this device is shown in Figure 3-35; it had a 1/8th inch diameter hole, was 1.9 inches long, and 0.8 inches in diameter. The quarter wave resonance was calculated to be 1780 Hz, while the measured fundamental was 1625 Hz with detectable second and third harmonics. End corrections for radiation from the openings is needed to bring the two frequencies in consonance. A second and third characteristic length is the diameter of the orifice $\mathbf{d_1}$ and the diameter of the tube $\mathbf{d_2}$. They determine the end corrections.

Fig 3-35. An acoustical diode.

Key **Points:** In most situations where a resonant cavity is in conjunction with a flow field, it does not contain mean flow {3.12.2}. Here, as with the corrugated pipe tone, the cavity contains both flow and sound. The most unique aspect of this device is that the tone sounds only with flow in one direction.

3.12.5 Thermal Sources

As noted in Chapter 2, fluctuating temperatures can be a source of sound. There are a number of Category II sources that occur in practical geometries. Most were discovered in the 19th century and are generally associated with resonant structures, such as tubes. The density change caused by heat release can be significant, so the generated sound field also can be significant.

Pieter Rijke (1812-1899), a Dutch physicist, heated a gauze material inside a vertical tube. The heat transferred to the air in the tube set it into near half-wave resonance. It is now called the *Rijke tube*. For a tube about one meter long and 3.5 cm in diameter, it was estimated that the power was equivalent to a loudspeaker with 1 kW of input at about 170 Hz. Originally, the gauze was heated with a Bunsen burner. Later, a wire grid was heated electrically. Heating cool air as it passes over the hot source sets the resonance when the phase (gauze/grid location) is correct. Warm air passing over cold wire grids will accomplishes the same objective.

What are the characteristic lengths and speeds? The characteristic length is heat source position **αL,** where **L** is the tube length. The characteristic speed must be that of the air flowing

over the heat source. That speed is the acoustic motion plus or minus the heated/cooled convection speed. References to this source can be found [4]. Since the resonance is about half-wave, the sound field is from two in-phase monopole-like sources, one at either tube end,

A gas flame inside a tube can drive resonance. It was also described in the 19th century and is called a s*inging flame.* The small fluctuations in gas flow from the burner are amplified by the resonance and with appropriate phase results in significant energy release and monopole-like sound from the tube.

Key Points: Heat release can be a potent source of sound. The few examples given above amplify the potential importance of heat transfer in creating sound sources.